

Research Paper

Theranostic pretargeted radioimmunotherapy of internalizing solid tumor antigens in human tumor xenografts in mice: Curative treatment of HER2-positive breast carcinoma

Sarah M. Cheal^{1,2}, Hong Xu³, Hong-fen Guo³, Mitesh Patel², Blesida Punzalan^{1,2}, Edward K. Fung⁴, Sang-gyu Lee⁴, Meghan Bell², Manisha Singh¹, Achim A. Jungbluth⁵, Pat B. Zanzonico⁴, Alessandra Piersigilli⁶, Steven M. Larson^{1,2}^{*}, Nai-Kong V. Cheung^{1,3}^{*}

1. Molecular Pharmacology Program, Memorial Sloan Kettering Cancer Center, New York, NY 10065, USA;
2. Department of Radiology, Memorial Sloan Kettering Cancer Center, New York, NY 10065, USA;
3. Department of Pediatrics, Memorial Sloan Kettering Cancer Center, New York, NY 10065, USA;
4. Department of Medical Physics, Memorial Sloan Kettering Cancer Center, New York, NY 10065, USA;
5. Department of Pathology, Memorial Sloan Kettering Cancer Center, New York, NY 10065, USA;
6. Tri-Institutional Laboratory of Comparative Pathology, Memorial Sloan Kettering Cancer Center, Weill Cornell Medicine, and The Rockefeller University, New York, NY 10065, USA.

*S.M.L and N.K.V.C are Co-PIs on this project.

 Corresponding author: S.M.L. (Phone: 646-888-2212; Fax: 646-717-3263; Email: larsons@mskcc.org).

© Ivyspring International Publisher. This is an open access article distributed under the terms of the Creative Commons Attribution (CC BY-NC) license (<https://creativecommons.org/licenses/by-nc/4.0/>). See <http://ivyspring.com/terms> for full terms and conditions.

Received: 2018.04.09; Accepted: 2018.07.24; Published: 2018.10.06

Abstract

In recent reports, we have shown that optimized pretargeted radioimmunotherapy (PRIT) based on molecularly engineered antibody conjugates and ¹⁷⁷Lu-DOTA chelate (DOTA-PRIT) can be used to cure mice bearing human solid tumor xenografts using antitumor antibodies to minimally internalizing membrane antigens, GPA33 (colon) and GD2 (neuroblastoma). However, many solid tumor membrane antigens are internalized after antibody binding and it is generally believed that internalizing tumor membrane antigens are not suitable targets for PRIT. In this study, we tested the hypothesis that DOTA-PRIT can be performed successfully to target HER2, an internalizing membrane antigen widely expressed in breast, ovarian, and gastroesophageal junction cancers.

Methods: DOTA-PRIT was carried out in athymic nude mice bearing BT-474 xenografts, a HER2-expressing human breast cancer, using a three-step dosing regimen consisting of sequential intravenous administrations of: 1) a bispecific IgG-scFv (210 kD) format (BsAb) carrying the IgG sequence of the anti-HER2 antibody trastuzumab and the scFv “C825” with high-affinity, hapten-binding antibody for Bn-DOTA (metal) (BsAb: anti-HER2-C825), 2) a 500 kD dextran-based clearing agent, followed by 3) ¹⁷⁷Lu-DOTA-Bn. At the time of treatment, athymic nude mice bearing established subcutaneous BT-474 tumors (medium- and smaller-sized tumors with tumor volumes of 209 ± 101 mm³ and ranging from palpable to 30 mm³, respectively), were studied along with controls. We studied single- and multi-dose regimens. For groups receiving fractionated treatment, we verified quantitative tumor targeting during each treatment cycle using non-invasive imaging with single-photon emission computed tomography/computed tomography (SPECT/CT).

Results: We achieved high therapeutic indices (TI, the ratio of radiation-absorbed dose in tumor to radiation-absorbed dose to critical organs, such as bone marrow) for targeting in blood (TI = 28) and kidney (TI = 7), while delivering average radiation-absorbed doses of 39.9 cGy/MBq to tumor. Based on dosimetry estimates, we implemented a curative fractionated therapeutic regimen for medium-sized tumors that would deliver approximately 70 Gy to tumors, which required treatment with a total of 167 MBq ¹⁷⁷Lu-DOTA-Bn/mouse (estimated absorbed tumor dose: 66 Gy). This regimen was well tolerated and achieved 100% complete responses (CRs; defined herein as tumor volume equal to or smaller than 4.2 mm³), including 62.5% histologic cure (5/8) and 37.5% microscopic residual disease (3/8) at 85 days (d). Treatment controls showed tumor progression to 207 ± 201% of pre-treatment volume at 85 d and no CRs. Finally, we show that treatment

with this curative ^{177}Lu regimen leads to a very low incidence of histopathologic abnormalities in critical organs such as bone marrow and kidney among survivors compared with non-treated controls.

Conclusion: Contrary to popular belief, we demonstrate that DOTA-PRIT can be successfully adapted to an internalizing antigen-antibody system such as HER2, with sufficient TIs and absorbed tumor doses to achieve a high probability of cures of established human breast cancer xenografts while sparing critical organs of significant radiotoxicity.

Key words: multistep targeting, bispecific antibodies, HER2, radioimmunotherapy, pretargeting, lutetium-177

Introduction

Radioimmunotherapy (RIT) with IgG as a radioactive carrier is generally ineffective when administered intravenously for treatment of solid tumors in humans. The problem is an unfavorable therapeutic index (TI), defined herein as the ratio of the radiation-absorbed dose to the tumor divided by the dose to radiosensitive tissue such as blood [1]. Hematological toxicity is typically dose-limiting for RIT. Alternatively, pretargeting RIT (PRIT) strategies may increase TIs by separating the antibody-mediated tumor targeting step from the administration of the cytotoxic radioligand in order to reduce the absorbed dose to radiosensitive tissues [2]. Herein, we adopt a bispecific antibody (BsAb)-based approach to PRIT, which utilizes a BsAb engineered to bind both a tumor-associated antigen and a radioactive hapten *in vivo*, with high affinity. For excellent reviews of BsAb-based PRIT, as well as alternative PRIT approaches, please refer to [3-6].

Using a pretargeting platform we call "DOTA-PRIT", we have demonstrated high TIs after parenteral injection in preclinical animal models of human carcinoma xenografts, achieving cures with minimal toxicity. The tumor antigen targets we selected were minimally internalizing membrane-expressed antigens of solid tumor, such as disialoganglioside (GD2 [7] on human neuroblastoma xenografts) and glycoprotein targets (GPA33 [8] on human colon cancer xenografts). In addition, the DOTA-PRIT approach was used by others to achieve high TI targeting in curative preclinical studies with CD20(+) [9] and CD38(+) [10] human xenografts.

DOTA-PRIT is based on a BsAb with nanomolar specificity for a tumor antigen and picomolar affinity for a low-molecular-weight hapten [11, 12]. The hapten is a radiometal complex of S-2-(4-aminobenzyl)-1,4,7,10-tetraazacyclododecane tetraacetic acid chelate ([M]-DOTA-Bn [13], e.g., as the β -emitter ^{177}Lu -DOTA-Bn). We have optimized the targeting of both the BsAb and the radiohapten through empirical testing in xenograft solid tumor models in mice. Initially, BsAb is administered at a dose designed to saturate the tumor receptor. After sufficient time has elapsed to permit tumor uptake of the non-radioactive BsAb, clearance of

non-tumor-bound BsAb is promoted with a dextran-based clearing agent (CA [14]). Subsequently, ^{177}Lu -DOTA-Bn is administered, which is captured by hapten binding to tumor-localized BsAb. Radioactivity not taken up by tumor is rapidly cleared from the body via the kidney [13].

Herein, we tested a variation of the DOTA-PRIT platform that targets HER2, an internalizing antigen [15] expressed by a wide spectrum of human cancers. Antibody-antigen systems that are internalized upon cell binding are considered sub-optimum for PRIT, since the effective concentration of cell-surface anti-hapten antibody domains are reduced as the antibody is internalized into the cell. *In vivo* internalization of the trastuzumab-HER2 complex has been previously demonstrated. For example, it was shown by Rudnick et al. that high-affinity radiolabeled forms of anti-HER2 antibodies (e.g., trastuzumab) were internalized and degraded *in vivo* by HER2-expressing tumors, thereby limiting their penetration of tumors [16]. For this reason, we emphasize *in vivo* studies to demonstrate anti-HER2-DOTA-PRIT. In the present study, our aims were to: (1) produce the novel anti-HER2-C825 BsAb to enable proof-of-concept studies with anti-HER2-DOTA-PRIT, (2) characterize the HER2(+) tumor cell surface internalization kinetics of the anti-HER2-C825 BsAb/HER2 antigen complex, (3) demonstrate highly specific tumor targeting of ^{177}Lu -DOTA-Bn with anti-HER2-DOTA-PRIT, and (4) test if TI was sufficient for safe and effective theranostic application of anti-HER2-DOTA-PRIT in mice bearing established subcutaneous (s.c.) human HER2(+) breast carcinoma xenografts.

Results

In vitro characterization of anti-HER2-C825 BsAb

Biochemical purity analysis of anti-HER2-C825 by size-exclusion high-pressure liquid chromatography (SE-HPLC) is shown in **Figure S1A**. SE-HPLC showed a major peak (96.5% by UV analysis) with an approximate molecular weight of 210 kD, as well as some minor peaks assumed to be

aggregates removable by gel filtration. The BsAb remained stable by SE-HPLC after multiple freeze and thaw cycles (data not shown).

The binding affinity to antigen BSA-(Y)-DOTA-Bn was measured by Biacore T100. Anti-HER2-C825 had a k_{on} of $2.10 \times 10^4 \text{ M}^{-1}\text{s}^{-1}$, a k_{off} of $1.25 \times 10^{-4} \text{ s}^{-1}$, and overall K_D of 6.0 nM—comparable to control BsAb huA33-C825 (k_{on} of $1.90 \times 10^4 \text{ M}^{-1}\text{s}^{-1}$, k_{off} of $2.20 \times 10^{-4} \text{ s}^{-1}$, and overall K_D of 11.6 nM; **Figure S1B**). The binding to tumor targets was measured by flow cytometry. Anti-HER2-C825 was equally efficient as parental trastuzumab in binding to the HER2(+) breast cancer cell line AU565 (**Figure S1C**). In summary, anti-HER2-C825 retained high binding capability to both targets (HER2 and DOTA-hapten).

Internalization kinetics and cellular processing of anti-HER2-C825

To characterize the internalization kinetics and cellular processing of anti-HER2-C825 by HER2(+) cells, anti-HER2-C825 was radioiodinated with iodine-131 (^{131}I) and *in vitro* cell binding studies were conducted with HER2(+) BT-474 cells up to 24 h at 37 °C. Cell surface ^{131}I -anti-HER2-C825 was rapidly internalized by BT-474 cells following incubation at 37 °C, with $25.6 \pm 1.16\%$ of the added radioactivity showing peak internalization at 2 h (**Figure 1**).

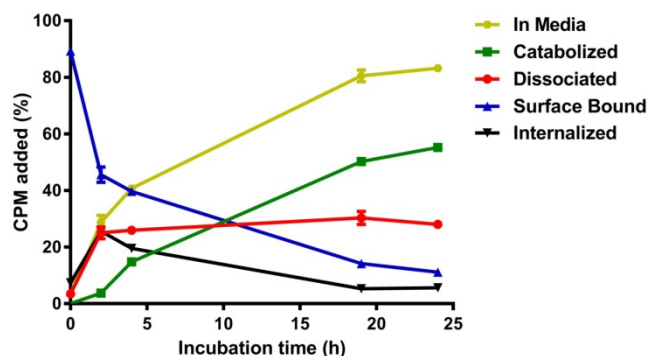


Figure 1. HER2(+) tumor surface-bound anti-HER2-C825 BsAb is rapidly internalized. Anti-HER2-C825 was radioiodinated and *in vitro* radiotracer binding studies were performed with HER2(+) BT-474 cells to determine the internalization and cellular processing at 37 °C of ^{131}I -anti-HER2-C825. Data is presented as mean \pm standard deviation (SD) ($n = 3$).

In addition, internalized radioactivity at 4 °C was on average ~ 15 -fold less than that of 37 °C when assayed at 4 h ($n = 6$; data not shown). At 37 °C from 2 to 24 h, the internalized radioactivity was observed to decrease on average by $\sim 80\%$ to $5.6 \pm 0.21\%$, suggesting the occurrence of intracellular processing and exocytosis. This was also apparent by the rate of increase in the percentage of catabolized radioactivity observed in the extracellular media (i.e., accumulation of low-molecular-weight catabolites), which showed a rate constant $K = 0.054 \text{ h}^{-1}$ and a half-time of 12.82 h ($R^2 = 0.995$). For the surface-bound activity fraction,

$\sim 50\%$ of the activity was lost in the first 2 h of incubation at 37 °C, while the remaining activity decayed with a half-life of 8.5 h ($R^2 = 0.992$). After incubation for 24 h (the time interval between BsAb and CA injections during DOTA-PRIT), $11.1 \pm 0.48\%$ of initially bound anti-HER2-C825 remained on the cell surface.

Control experiments to assay the *in vitro* stability of ^{131}I -anti-HER2-C825 in media at 37 °C from 0 to 24 h showed that the percent change in antibody-associated radioactivity between those two time points was -2.1% , suggesting that the observed catabolized activity in the extracellular media fraction was primarily due to internalization and exocytosis of ^{131}I -anti-HER2-C825.

Demonstration of *in vivo* anti-HER2 DOTA-PRIT

The optimized doses of BsAb and CA for *in vivo* anti-HER2 DOTA-PRIT were empirically determined to be 0.25 mg (1.19 nmol) and 62.5 μg (0.125 nmol of dextran; 7.63 nmol of (Y)-DOTA-Bn), respectively, using groups of BT-474 tumor-bearing mice. The time intervals between injections (24 h between BsAb and CA, and 4 h between CA and ^{177}Lu -DOTA-Bn) were based on previous DOTA-PRIT studies [7, 8] and not varied during this study. No attempts were made to exclude the CA in the dosing regimen, as this would require long time intervals between BsAb and hapten administration in order to sufficiently reduce circulating BsAb. At the same time, this would also reduce the concentration of surface-bound anti-hapten C825 scFv antibody due to *in vivo* internalization of the BsAb-trastuzumab-HER2 complex. Also, it was reported that the C825 antibody is susceptible to loss of DOTA-hapten binding capacity following prolonged incubation in 50% mouse serum [12]. Mass ranges of 0.25-0.75 mg BsAb/mouse (1.19-3.57 nmol/mouse) and 18.75-70 μg CA/mouse (0.0375-0.14 nmol of dextran; 2.29-8.54 nmol of (Y)-DOTA-Bn) were used for optimization. A summary of select biodistribution data from these optimization efforts is provided in **Figure 2**, while remaining data are presented in **Figure S2** and **Table S1**.

This targeting regimen led to tumor uptake (as percent injected activity per gram, %IA/g; mean \pm standard error of the mean (SEM)) at 24 h post-injection (p.i.) of $7.58 \pm 0.78 \text{ \%IA/g}$, with the kidneys having the highest normal uptake ($0.73 \pm 0.05 \text{ \%IA/g}$). Notably, without administration of the CA-step (i.e., with anti-HER2-C825 given at $t = -28 \text{ h}$ followed by ^{177}Lu -DOTA-Bn at $t = 0 \text{ h}$), both tumor and blood uptake of ^{177}Lu activity at 24 h p.i. was much higher, $19.94 \pm 3.54 \text{ \%IA/g}$ and 4.95 ± 1.17

%IA/g, respectively, consequently leading to unfavorable tumor-to-blood ratios (T/B; T/B: 4.0 ± 1.2) (Figure 2). With optimized CA dose of 62.5 μg (0.125 nmol of dextran; 7.63 nmol of (Y)-DOTA-Bn), the average uptake for tumor and blood was reduced by ~60% (for tumor, from ~20 to 7.6 %IA/g) or ~95% (for blood, from ~5 to 0.3 %IA/g), respectively, compared with no CA control. In summary, use of the CA step significantly improved the tumor-to-blood ratio at 24 h p.i. of ^{177}Lu -DOTA-Bn (T/B: 26.7 ± 9.0) compared with no CA control, but at the expense of lower tumor uptake.

To demonstrate HER2-specific targeting, biodistribution studies were performed in mice bearing s.c. HER2(-) MDA-MB-468. Tumor uptake of pretargeted ^{177}Lu activity at 24 h p.i. in HER2(-) tumors was ~7-fold lower (2.75 ± 0.17 %IA/g) than in HER2(+) BT-474 tumors (19.94 ± 1.7 %IA/g) (Figure 2). In addition, injection of BT-474 tumor-bearing animals with ^{177}Lu -DOTA-Bn alone (i.e., no PRIT control) showed negligible uptake in tumor at 24 h p.i. (0.07 ± 0.01 %IA/g), as well as minimal uptake in blood (0.002 ± 0.00 %IA/g) and kidney (0.38 ± 0.01 %IA/g), demonstrating that ^{177}Lu -DOTA-Bn has

minimal whole-body retention due to rapid renal clearance (Table S2).

Serial biodistribution-based dosimetry

Using the optimized anti-HER2-DOTA-PRIT regimen, serial biodistribution studies were performed at various times from 1-336 h p.i. in BT-474 tumor-bearing mice to determine the time of peak tumor uptake and calculate dosimetry for subsequent therapy studies. As shown in Figure 3, peak tumor uptake of pretargeted ^{177}Lu activity (~5.6 MBq/~30 pmol) was observed at 24 h p.i. to be 7.58 ± 0.78 %IA/g, with corresponding activities of 0.28 ± 0.09 %IA/g for blood (T/B: 26.7 ± 9.0) and 0.73 ± 0.05 %IA/g for kidney (tumor-to-kidney ratio (T/K): 10.4 ± 1.3). Also, ^{177}Lu activity in tumor remained relatively constant from 1-24 h p.i., ranging from ~5 to 8 %IA/g, suggesting that tumor targeting was very rapid, and that biologic clearance of activity from tumor was relatively slow. The tumor activity dropped to 2.29 ± 0.41 %IA/g and 0.32 ± 0.06 %IA/g at 96 and 336 h p.i., respectively, leading to an approximate tumor clearance half-life of 38.6 h ($R^2 = 0.894$).

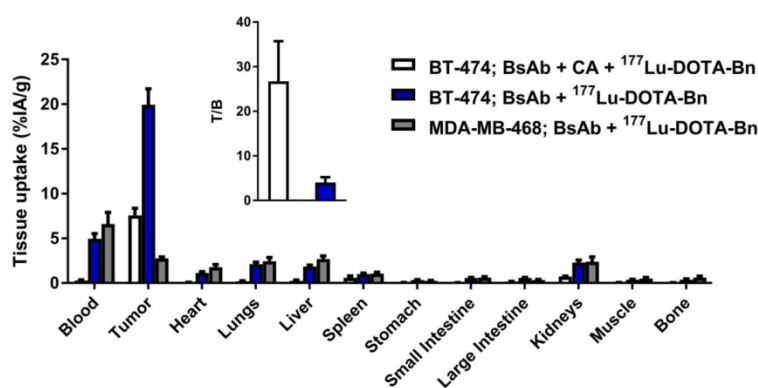


Figure 2. *In vivo* investigation of anti-HER2 DOTA-PRIT with and without the CA step, as well as in HER2-positive (BT-474) and HER2-negative (MDA-MB-468) human breast carcinoma mouse models. Biodistribution data at 24 h p.i. of ^{177}Lu -DOTA-Bn (~5.6 MBq, 30 pmol) demonstrating HER2(+) tumor-specific targeting with high T/B. BsAb dose was 0.25 mg/1.19 nmol for all groups. The CA dose was 62.5 μg (0.125 nmol of dextran; 7.63 nmol of (Y)-DOTA-Bn) for the group given anti-HER2 DOTA-PRIT with the CA step. Groups of athymic nude mice bearing either s.c. HER2(+) (BT-474) or s.c. HER2(-) (MDA-MB-468) tumors were used. All tumors ranged from 100-200 mg *ex vivo*. n.d.: not determined; Int.: intestine. Data is presented as %IA/g (mean \pm SEM). Data is also provided in tabular form in Table S2.

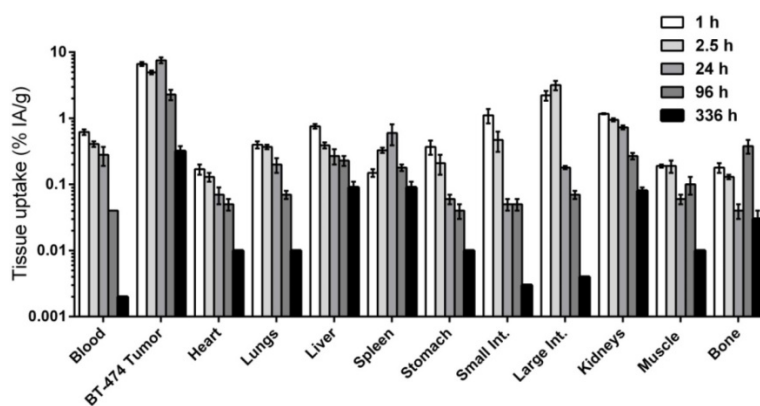


Figure 3. Serial *in vivo* biodistribution studies with anti-HER2-DOTA-PRIT. Very high tumor targeting of ^{177}Lu activity with minimal uptake in normal tissues, including blood and kidney, was seen as early as 1 h p.i. Serial biodistribution data from 1-336 h p.i. of pretargeted ^{177}Lu -DOTA-Bn 5.5-6.1 MBq (~30 pmol) showing tissue uptake (as %IA/g; note: log-scale for y-axis) in s.c. BT-474 tumor and select normal tissues. Data for 24 h p.i., during which tumor uptake was maximum, is also provided in Figure 2. Data for all time points studied are provided in tabular form in Table S3. Int.: intestine.

Absorbed dose estimates were obtained for tumor and normal tissues assayed by biodistribution in order to guide therapy studies and predict the dose-limiting tissue. As shown in **Table 2**, the estimated absorbed doses of ^{177}Lu -DOTA-Bn (as cGy/MBq) for blood, tumor, liver, spleen, and kidney were 1.4, 39.9, 3.3, 0.3, and 5.6, respectively. The estimated dose to the kidneys was the highest among normal tissues, leading to a TI of 7. Based on estimated maximum tolerated doses of 250 and 2000 cGy for blood (bone marrow) and kidney, respectively [17], the estimated maximum tolerated activity is ~180 MBq, with blood (bone marrow) as the dose-limiting tissue (TI for blood: 28).

Table 2. Estimated absorbed doses for optimized anti-HER2-DOTA-PRIT with ^{177}Lu -DOTA-Bn in nude mice carrying s.c. HER2(+) BT-474 tumors, based on serial biodistribution data from 1.0-336 h p.i. of ^{177}Lu -DOTA-Bn (30 pmol).

Tissue	^{177}Lu -DOTA-Bn (cGy/MBq)	^{177}Lu -therapy Therapeutic Index
Blood	1.4	28
Tumor	39.9	
Heart	0.4	100
Lung	1.3	31
Liver	3.3	12
Spleen	0.3	133
Stomach	0.3	133
Small Intestine	0.4	100
Large Intestine	0.8	50
Kidneys	5.6	7
Muscle	0.9	44
Bone	0.7	57

Investigation of the influence of mass of radiolabeled DOTA on tumor and normal tissue uptake in anticipation of therapeutic dosing

Prior to therapy studies, an *in vivo* study was conducted with a group of BT-474 tumor-bearing mice given optimized anti-HER2-DOTA-PRIT in conjunction with a therapeutic amount of injected activity (IA) of ^{177}Lu -DOTA-Bn (~56 MBq, 300 pmol), as opposed to the lower tracer administered activity of ^{177}Lu -DOTA-Bn (~5.6 MBq, 30 pmol) used during optimization and dosimetry studies. These animals were imaged using SPECT/CT at 24 h p.i. and biodistribution was assessed immediately following imaging to determine the influence of administered mass of radiolabeled DOTA on tumor and normal tissue uptake at 24 h p.i. The images clearly revealed tumor delineation in the lower flank at 24 h p.i. of ^{177}Lu -DOTA-Bn (**Figure S3**), suggesting high absolute tumor uptake, as well as high T/B. Biodistribution revealed tumor, blood, and kidney uptake of $5.53 \pm$

$0.27\% \text{IA/g}$, $0.29 \pm 0.05\% \text{IA/g}$, and $0.56 \pm 0.08\% \text{IA/g}$, respectively (**Figure 4**), suggesting that high TIs would be maintained for critical tissues during therapeutic dosing. For the higher administered dose of 300 pmol, there were only very slight differences between tumor and kidney uptake observed ($7.58 \pm 0.78\% \text{IA/g}$ versus $5.53 \pm 0.27\% \text{IA/g}$, Student's t-test $P = 0.051$; and $0.73 \pm 0.05\% \text{IA/g}$ versus $0.56 \pm 0.08\% \text{IA/g}$, Student's t-test $P = 0.044$; for tumor and kidney, respectively) compared with the group given 30 pmol. Nonetheless, the T/K ratio was almost identical (~10) for both doses. Therefore, we assume no major effects of radiolabeled DOTA mass on radiation doses and TIs during therapeutic (i.e., 300 pmol) dosing.

Intratumoral distributions of BsAb and pretargeted ^{177}Lu activity

The intratumoral BsAb targeting and its relationship with HER2 expression, as well as the tumor microdistribution of pretargeted ^{177}Lu activity, was investigated using immunohistochemistry (IHC) and autoradiography with excised medium-sized BT-474 tumors at 24 h p.i. of BsAb or pretargeted ^{177}Lu -DOTA-Bn, respectively. These studies revealed somewhat heterogeneous uptake of BsAb in HER2(+) tumor regions in the larger-sized tumor, but relatively uniform and homogeneous tumor distribution of pretargeted ^{177}Lu activity in the smaller-sized tumor (**Figure 5**). Overall, particularly for medium-sized BT-474 tumors (average pre-treatment tumor volume: ~100 mm³), this supports utilizing beta-emitting therapeutic radionuclides for therapy, which have relatively long tissue penetration ranges to compensate for heterogeneity, as bystander tumors with limited antigen expression in the region of the targeted molecule may be eradicated (e.g., the mean penetration range of β^- particles emitted by ^{177}Lu in soft tissue is ~0.7 mm).

Therapy studies

Therapy studies were carried out to determine the effect of estimated tumor dose on response for a wide range of starting tumor sizes, as well as the feasibility of achieving a high probability of cures, particularly with dosimetry-based treatment planning with estimated absorbed tumor doses of ~70 Gy. A summary of the three anti-HER2-DOTA-PRIT therapy studies is provided in **Table 3**. Notably, during the first two studies of single-cycle treatment, the tumor doubling time in the absence of treatment was quite rapid (~7 days), but for an unknown reason, was much slower during the third study when fractionated treatment was investigated (> 50 days in some animals).

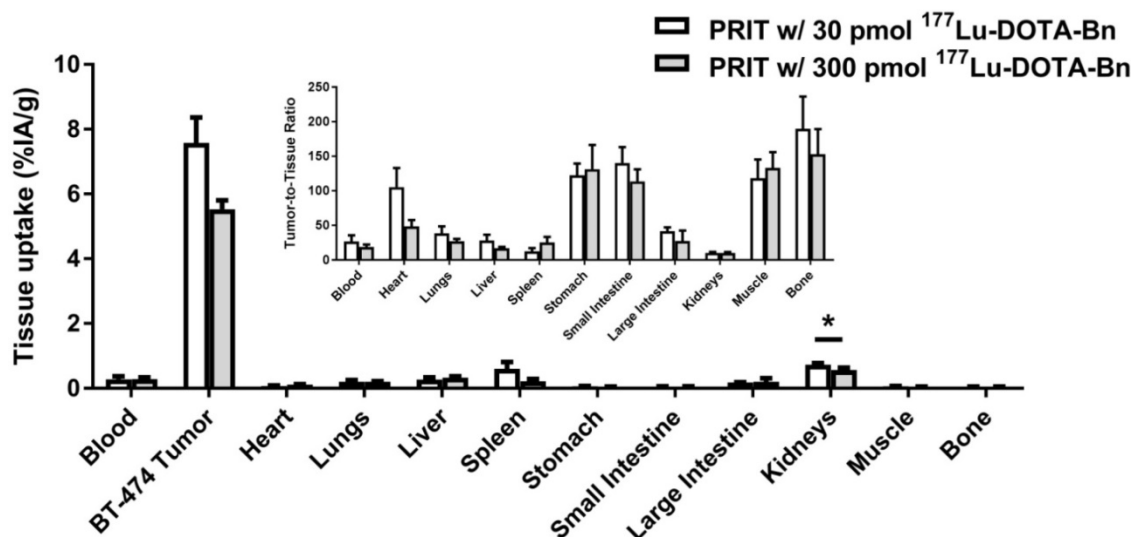


Figure 4. Comparison of biodistribution studies at 24 h p.i. of injection with two different administered doses of ¹⁷⁷Lu-DOTA-Bn hapten (30 pmol versus 300 pmol). Please see Table S4 for biodistribution data in tabular form. *Denotes statistical significance.

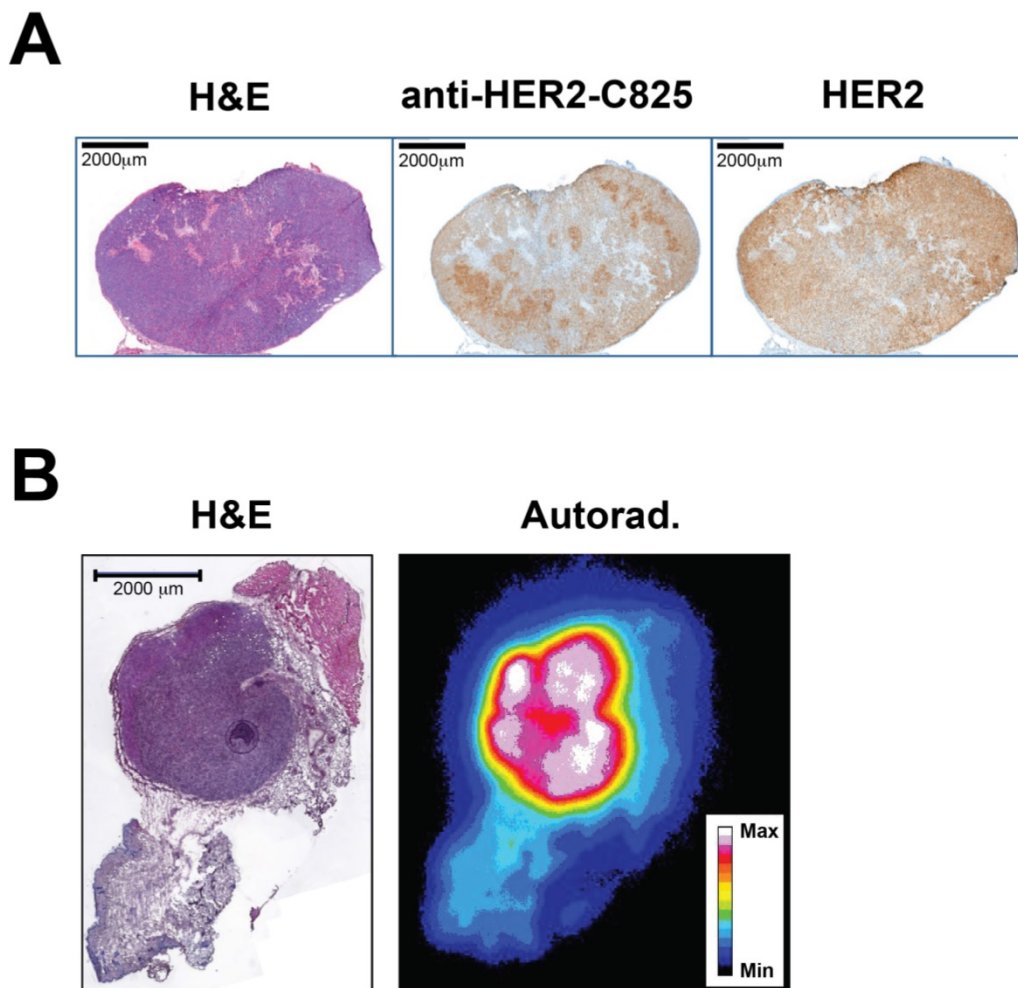


Figure 5. Representative histology, immunohistochemistry (IHC), and autoradiography (Autorad.) to assay the BT-474 intratumoral distribution of BsAb and pretargeted ¹⁷⁷Lu activity. (A) IHC at 24 h p.i. of anti-HER2-C825 BsAb (0.25 mg, 1.19 nmol). Scale bar is 2000 µm. Using image-based densitometry, the % positive area of BsAb IHC and HER2 IHC was 51% and 61%, respectively, for a ratio of (BsAb IHC)/(HER2 IHC) of 0.84. (B) Hematoxylin and eosin (H&E) stain and autoradiography of pretargeted ¹⁷⁷Lu-DOTA-Bn (55.5 MBq, 300 pmol) at 24 h p.i. Scale bar is 2000 µm. Max: maximum, Min: minimum.

Table 3. Summary of anti-HER2-DOTA-PRIT efficacy and toxicity studies.

DOTA-PRIT treatment (number of mice/group)	Control groups (number of mice/group)	Tumor sizes (range, mm ³)	Tumor dose (Gy)	Blood dose (Gy)	Kidney dose (Gy)	Median survival ^a	Therapeutic outcome/study endpoint
Single-cycle treatment with 55.5 MBq (5)	No treatment (5); BsAb only (5); 55.5 MBq of ¹⁷⁷ Lu-DOTA-Bn alone (5)	Small; palpable-30	22	0.8	0.3	No treatment: 7 d; BsAb only: 16 d, 55.5 MBq of ¹⁷⁷ Lu-DOTA-Bn alone: 7 d, and undefined for 55.5 MBq.	No CRs in no treatment or 55.5 MBq of ¹⁷⁷ Lu-DOTA-Bn alone; BsAb only: 1/5 CR and 1/1 cure/85 d. For 55.5 MBq 5/5 CR, and 3/4 cures/85 d
Single-cycle treatment with 11.1, 33.3 or 55.5 MBq (5)	No treatment (5); 33.3 MBq of ¹⁷⁷ Lu-DOTA-Bn alone (5)	Medium; ~100-400	4.4, 13, or 22	0.2, 0.5, or 0.8	0.6, 1.9, or 3.1	No treatment: 6 d; 33.3 MBq of ¹⁷⁷ Lu-DOTA-Bn alone: 25 d; for 11.1 MBq: 21 d; for 33.3 MBq: 42 d; for 55.5 MBq: 108 d.	No CRs in no treatment or 33.3 MBq of ¹⁷⁷ Lu-DOTA-Bn alone; for 11.1 MBq: 1/5 CR, and 1/5 regression to palpable; for 33.3 MBq: 0/5 CR; for 55.5 MBq: 1/5 CR. Overall: 2/15 CR and 1/15 regression to palpable; 2/6 cures/200 d
Triple-cycle fractionated treatment with 55.5 MBq (total IA: ~167 MBq) (8)	No treatment (6); BsAb only (5); IgG-DOTA-PRIT (6)	Medium; ~100-400	66	2.3	9.3	No treatment: 35.5 d; BsAb only: 18 d; control IgG-DOTA-PRIT: 30 d; anti-HER2-DOTA-PRIT: undefined.	No CRs in controls; 2/8 CR, 6/8 regression to palpable, 5/8 cures/85 d

^aSurvival was defined as time to tumor doubling or death by any other cause.

^bOne each in 11.1 and 55.5 MBq DOTA-PRIT-treated groups.

^cTotal BsAb mass administered per mouse was 0.75 mg (3.57 nmol).

Small tumors, single cycle: Shown in **Figure 6A**, single-cycle anti-HER2-DOTA-PRIT with 55.5 MBq ¹⁷⁷Lu-DOTA-Bn (estimated delivered absorbed tumor dose: 22 Gy) was effective in treating small s.c. xenografts, resulting in a high frequency of complete responses (CRs) (5/5, 100%) with no recurrence observed in any animals to 85 d when survivors (4/5, 80%) were submitted for necropsy. All tumors were observed to completely disappear, with the exception of a single treated mouse with a starting tumor volume of 24 mm³, which showed CR to a palpable mass. Planar scintigraphy of groups of mice undergoing either anti-HER2-DOTA-PRIT or treatment with only 55.5 MBq of ¹⁷⁷Lu-DOTA-Bn clearly showed pretargeting-specific tumor uptake at 20 h p.i., which persisted in tumor until at least 70 h p.i. (**Figure S4**). Tumor response in control groups was generally not seen and tumors showed progression with no CRs, with the exception of a single mouse in the BsAb only group that showed tumor shrinkage to CR at ~40 d post-treatment with no subsequent recurrence (1/5, 20%). On Day 40 post-treatment, differences in tumor volumes for control groups were not statistically significant (data not shown). In addition, at 85 d, tumor sizes for control groups progressed on average to 350-3130% of pre-treatment volumes, with animals treated with BsAb only showing the least average progression. Median survival was 7 d for no treatment, 16 d for BsAb, 7 d for 55.5 MBq of ¹⁷⁷Lu-DOTA-Bn only, and undefined for anti-HER2-DOTA-PRIT + 55.5 MBq of ¹⁷⁷Lu-DOTA-Bn. During survival analysis (Log-rank, Mantel-Cox), a significant difference was found between no treatment and those treated with BsAb only ($P = 0.0495$), reflecting tumor response to the

BsAb (trastuzumab) treatment. On the other hand, no significant difference was seen for no treatment versus 55.5 MBq of ¹⁷⁷Lu-DOTA-Bn only ($P = 0.1336$), consistent with lack of tumor localization of ¹⁷⁷Lu activity in the absence of pretargeting as seen in the planar scintigraphy imaging (**Figure S4**). As expected, significant differences were seen in median survival for anti-HER2 DOTA-PRIT + 55.5 MBq versus all other groups ($P = 0.0015-0.0144$).

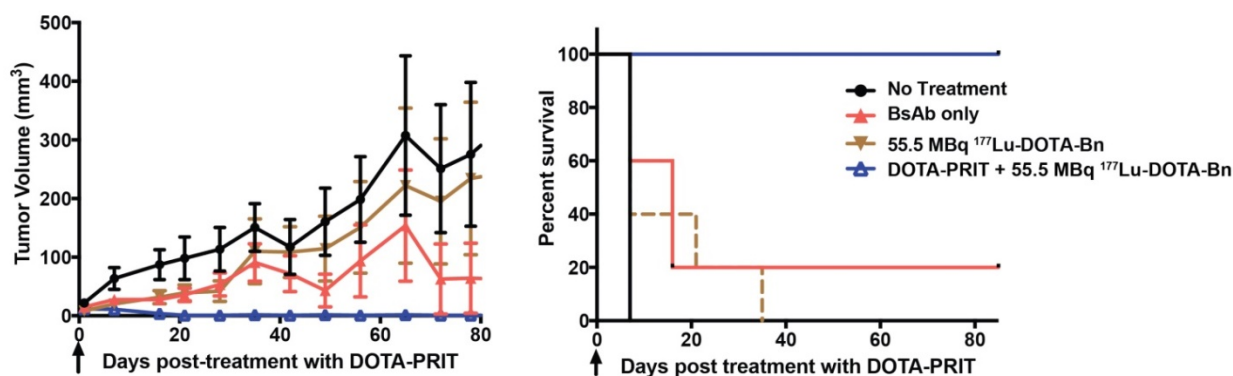
Medium tumors, single cycle: Treatment of mice bearing medium-sized s.c. xenografts with single-cycle anti-HER2-DOTA-PRIT with 11.1-55.5 MBq of ¹⁷⁷Lu-DOTA-Bn did not produce generally remarkable tumor responses compared to controls, suggesting that estimated absorbed tumor doses of 4.4-22 Gy were insufficient for producing a high probability of tumor CR (**Figure 6B**). On day 40 post-treatment, the difference between tumor volumes for control and treatment groups was not statistically significant (data not shown). Later, on day 80 post-treatment, there were statistically significant differences between surviving controls (non-treated and those treated with 33.3 MBq of ¹⁷⁷Lu-DOTA-Bn only; $n = 6$, range: 382-916 mm³) and the 11.1 and 55.5 MBq treatment groups, thus suggesting therapeutic efficacy and survival benefit—for 11.1 MBq, $n = 5$, range: palpable-544 mm³, Student's t-test $P = 0.013$ with palpable defined as 4.2 mm³; for 33.3 MBq, $n = 3$, range: 45-777 mm³, Student's t-test $P = 0.282$; for 55.5 MBq, $n = 3$, range: 8-159 mm³, Student's t-test $P = 0.004$. Median survival was 6 d for no treatment, 25 d for 33.3 MBq of ¹⁷⁷Lu-DOTA-Bn only, 21 d for anti-HER2-DOTA-PRIT + 11.1 MBq of ¹⁷⁷Lu-DOTA-Bn, 42 d for anti-HER2-DOTA-PRIT + 33.3 MBq of ¹⁷⁷Lu-DOTA-Bn, and 108 d for

anti-HER2-DOTA-PRIT + 55.5 MBq of ^{177}Lu -DOTA-Bn. During survival analysis (Log-rank, Mantel-Cox), no significant differences were found between no treatment and treatment with 33.3 MBq of ^{177}Lu -DOTA-Bn only ($P = 0.081$), but significant differences were seen between no treatment and 11.1 MBq ($P = 0.004$), no treatment and 33.3 MBq ($P = 0.009$), and no treatment and 55.5 MBq ($P = 0.013$). When comparing DOTA-PRIT treatment groups, no significant differences were seen for 11.1 MBq versus 33.3 MBq ($P = 0.754$), 11.1 MBq versus 55.5 MBq ($P = 0.782$), and 33.3 MBq versus 55.5 MBq. A small proportion of animals treated with anti-HER2-DOTA-PRIT, irrespective of treatment IA (2/15, 11.1%), showed CRs by ~75-100 d post-treatment (1/5 from the 11.1 MBq and 55.5 MBq groups); this was most likely due to the effect of the trastuzumab-like action of the BsAb.

Medium tumors, three cycles: Although single-cycle treatment was ineffective in treating medium-sized tumors, fractionated delivery of a greater tumor-absorbed radiation dose showed to be

highly effective. Treatment of groups of mice bearing medium-sized s.c. xenografts with three cycles of anti-HER2-DOTA-PRIT plus ^{177}Lu -DOTA-Bn (55.5 MBq/cycle, estimated delivered absorbed tumor dose: 66 Gy) led to 100% CRs (8/8), whereas tumor progression with no CRs were observed in the treatment controls (**Figure 7A**). Specifically, 2/8 treated animals showed complete tumor disappearance (25%), while 6/8 showed regression to palpation threshold (75%). Tumor volumes at 85 d for control non-treated, BsAb treated, or control IgG-DOTA-PRIT groups were $134 \pm 89\%$, $396 \pm 252\%$, and $114 \pm 155\%$ of pre-treatment volume, respectively. Median survival was 35.5 d for no treatment, 18 d for BsAb, 30 d for control IgG-DOTA-PRIT, and undefined (prefer >100 d) for anti-HER2-DOTA-PRIT. During survival analysis (Log-rank, Mantel-Cox), no significant differences were found between no treatment and those treated with BsAb only ($P = 0.178$), suggesting that the therapeutic effect of the trastuzumab-like action of the BsAb was less effective in mice bearing medium-sized tumors, in contrast to

A Single-cycle therapy, small-sized tumors



B Single-cycle therapy, medium-sized tumors

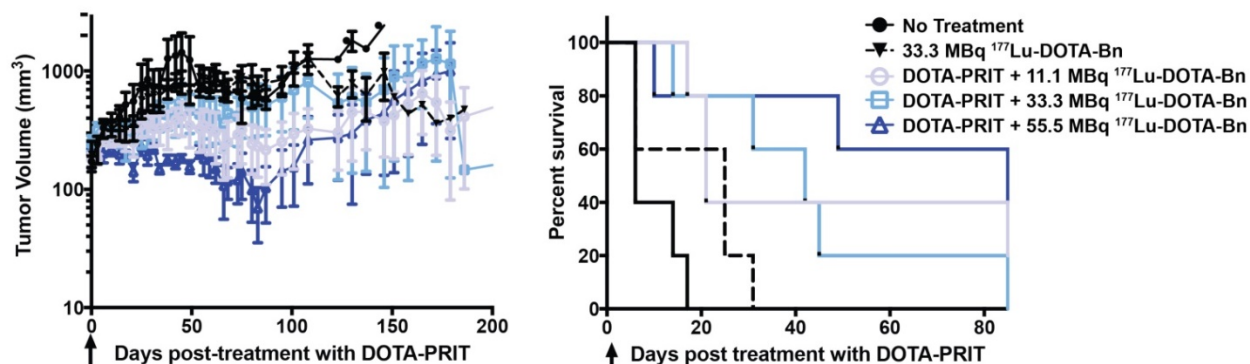


Figure 6. Single-cycle anti-HER2-DOTA-PRIT with IA of 55.5 MBq leads to CRs in mice with small-sized BT-474 tumors, but is generally ineffective in mice bearing medium-sized BT-474 tumors. Tumor volumes are presented as mean \pm SEM. Black arrow indicates the day of ^{177}Lu -DOTA-Bn injection. Survival was defined as time to tumor doubling and included deaths from other causes. (A) Treatment of mice bearing small-sized tumors with single-cycle anti-HER2-DOTA-PRIT + 55.5 MBq of ^{177}Lu -DOTA-Bn versus control groups. Median survival was 7 d for no treatment, 16 d for BsAb, 7 d for 55.5 MBq of ^{177}Lu -DOTA-Bn only, and undefined for anti-HER2-DOTA-PRIT + 55.5 MBq of ^{177}Lu -DOTA-Bn. (B) Treatment of mice bearing medium-sized tumors with single-cycle anti-HER2-DOTA-PRIT + 11.1, 33.3, or 55.5 MBq of ^{177}Lu -DOTA-Bn versus control groups. Median survival was 6 d for no treatment, 25 d for 33.3 MBq of ^{177}Lu -DOTA-Bn only, 21 d for anti-HER2-DOTA-PRIT + 11.1 MBq of ^{177}Lu -DOTA-Bn, 42 d for anti-HER2-DOTA-PRIT + 33.3 MBq of ^{177}Lu -DOTA-Bn, and 108 d for anti-HER2-DOTA-PRIT + 55.5 MBq of ^{177}Lu -DOTA-Bn.

what was seen in mice bearing smaller-sized tumors. Also, no significant difference was seen between no treatment and control IgG-DOTA-PRIT ($P = 0.836$) and no significant difference was seen between BsAb and control IgG-DOTA-PRIT ($P = 0.265$). Significant differences were seen between anti-HER2-DOTA-PRIT and no treatment, BsAb, and control IgG-DOTA-PRIT ($P = 0.0010$, 0.0001 , and 0.0066 , respectively).

SPECT/CT was conducted on select mice undergoing fractionated treatment to verify and quantify tumor uptake. As shown in **Figure 8A**, imaging of randomly selected mice at 24 h p.i. of cycle 1 ^{177}Lu -DOTA-Bn pretargeted with either control IgG-DOTA-PRIT or anti-HER2-DOTA-PRIT showed anti-HER2-C825 tumor-specific targeting of radioactivity, with negligible tumor uptake during

control IgG-DOTA-PRIT. Also, three randomly selected mice undergoing fractionated anti-HER2-DOTA-PRIT were serially imaged with SPECT/CT. Representative images for one of the animals at 24 h p.i. of cycles 1, 2, and 3 of ^{177}Lu -DOTA-Bn are provided in **Figure 8B**, while the data for the other two mice are provided in **Figure S6**. Image-derived region-of-interest (ROI) analysis of the tumor region was also conducted, and a graph displaying the tumor ^{177}Lu activities (expressed as MBq per cc of tumor; MBq/cc) during each cycle of treatment as a function of time (h) post-cycle 1 treatment start is also provided in **Figure 8B**, which shows that the average tumor uptake ranged from ~ 4.3 to 6.1 MBq/cc 24 h following each treatment cycle injection of ^{177}Lu -DOTA-Bn.

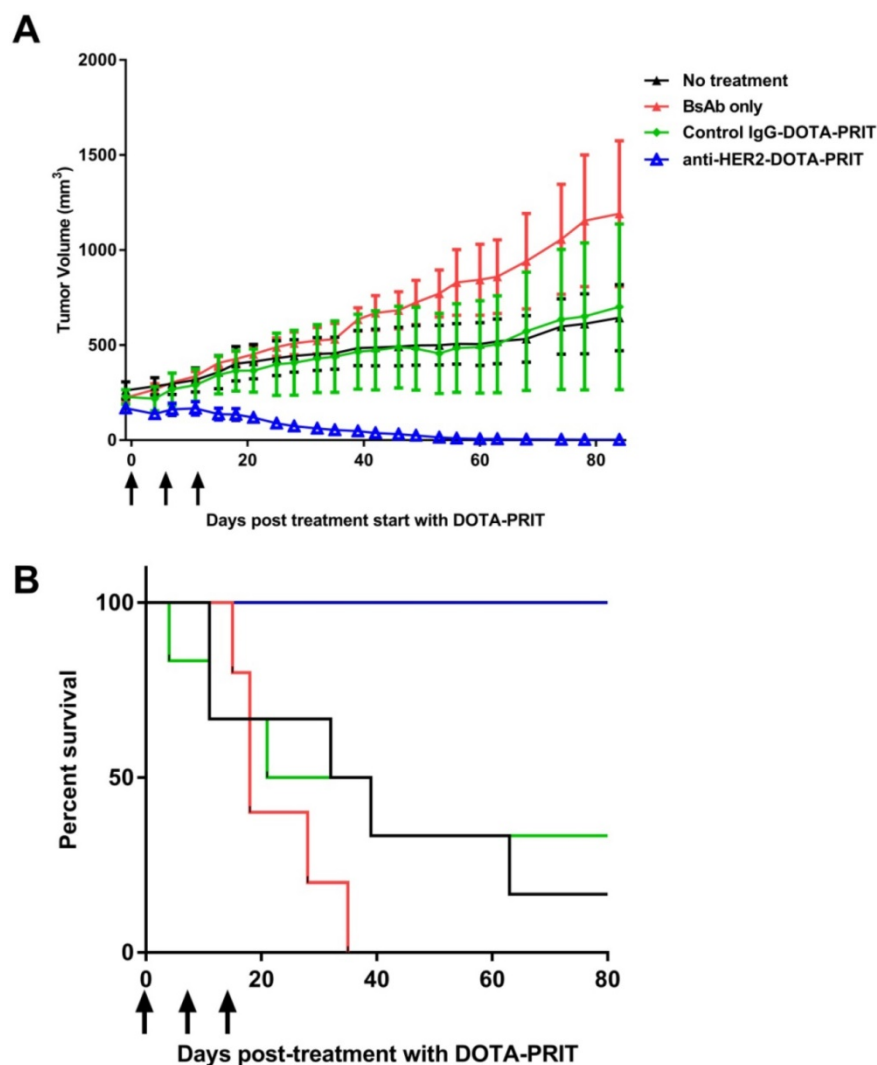


Figure 7. Fractionated anti-HER2-DOTA-PRIT with IA of 167 MBq led to 100% regression to palpable CRs (8/8) in mice with medium-sized xenografts at treatment initiation, with no recurrence at 85 d. (A) Tumor response curves for the four treatment arms presented as mean \pm SEM. Black arrows indicate day of injection of ^{177}Lu -DOTA-Bn. (B) Survival analysis of fractionated treatment. Survival was defined as time to tumor doubling and included deaths from other causes. Median survival was 35.5 d for no treatment, 18 d for BsAb, 30 d for control IgG-DOTA-PRIT, and undefined (prefer > 80 d) for anti-HER2-DOTA-PRIT.

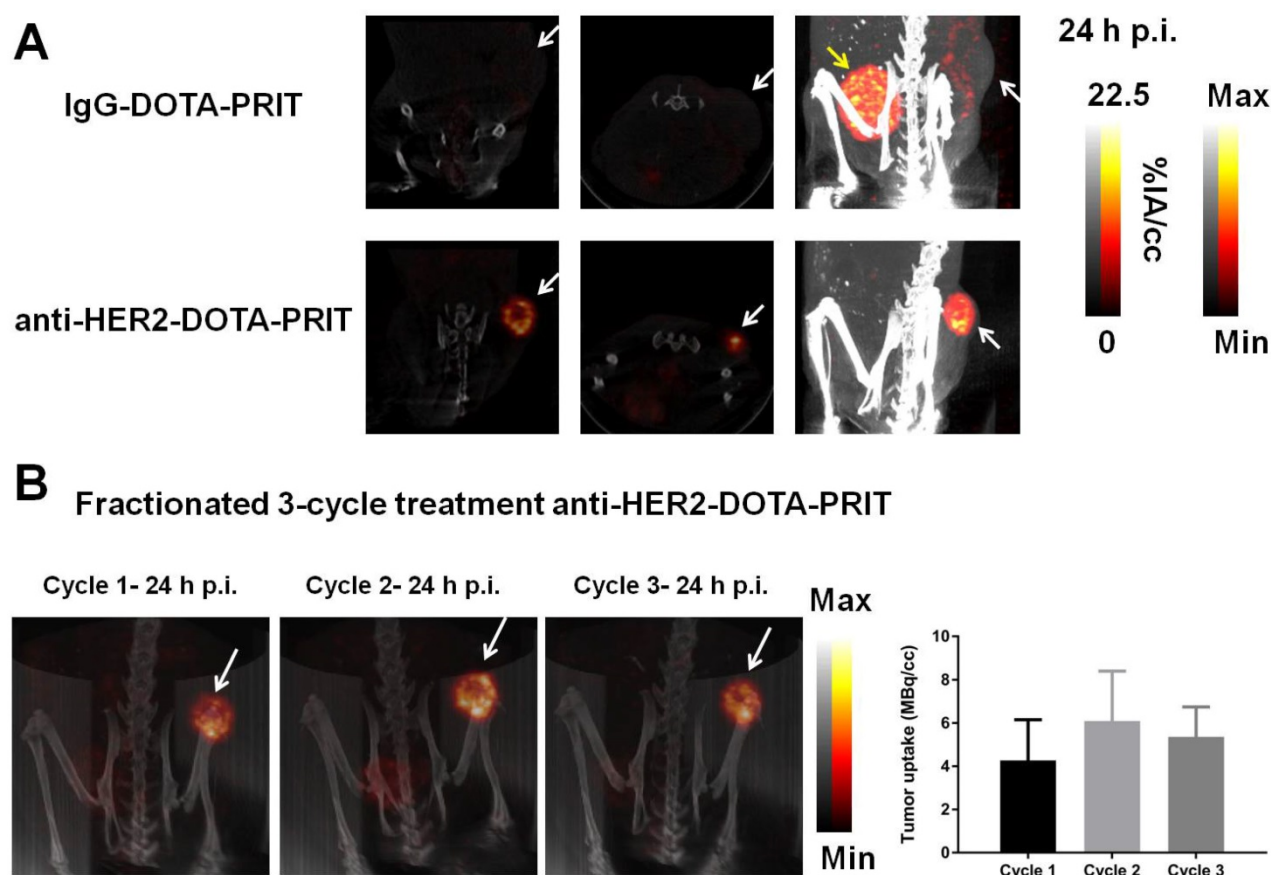


Figure 8. SPECT/CT monitoring of fractionated anti-HER2-DOTA-PRIT treatment. The imaging field-of-view was limited to the caudal half of the animal (midline to tail) to center on the tumor (white arrow). The bladder is indicated when appropriate by a yellow arrow. **(A)** Representative SPECT/CT images of BT-474 tumor-bearing animals 24 h p.i. of cycle 1 ^{177}Lu -DOTA-Bn (55.5 MBq, 300 pmol) pretargeted with either control IgG-DOTA-PRIT or anti-HER2-DOTA-PRIT (from left to right: coronal and transverse slices through center of tumor, maximum intensity projection (MIP)). For the IgG-DOTA-PRIT mouse, the tumor ROI was 0.46 ± 0.33 MBq/cc (mean \pm SD), with min-max of 0.00-2.92 MBq/cc. For the anti-HER2-DOTA-PRIT mouse, the tumor ROI was 5.24 ± 2.87 MBq/cc (mean \pm SD), with min-max of 0.069-19.75 MBq/cc. **(B)** Representative serial SPECT/CT MIP images of a BT-474 tumor-bearing animal undergoing fractionated anti-HER2-DOTA-PRIT (left), taken 24 h p.i. of each cycle of radioactive injection. The image-derived region-of-interest (ROI) values for tumor uptake at 24 h p.i. of cycle 1, 2, or 3 ^{177}Lu -DOTA-Bn (55.5 MBq, 300 pmol) are presented as MBq/cc (mean \pm SD).

Toxicity

In summary, during each of the therapy experiments, no significant average weight loss was seen in any of the treatment groups compared with controls (Figures S5 and Figure S7). Notably, no acute toxicity was seen for the fractionated anti-HER2-DOTA-PRIT regimen with 55.5 MBq of ^{177}Lu -DOTA-Bn/cycle (Figure S7), suggesting that more aggressive treatment regimens could be safely utilized. Tables S5-S7 summarize the criteria for removal from each therapy experiment. These included: (1) euthanasia needed due to excessive weight loss, (2) death of the animal, and (3) euthanasia needed due to excessive tumor burden. In this BT-474 animal model, we observed that a few animals showed rapid deterioration, irrespective of treatment regimen (including non-treated controls), presumably related to known effects of treatment with implantable estrogen pellets (e.g., urinary retention [18] and endometrial hyperplasia [19]). Therefore, during the fractionated treatment study, three

randomly selected animals that exhibited rapid weight loss within 12-22 d post-treatment start were submitted for full necropsy to determine the cause of poor clinical condition (one from each treatment group: no treatment, BsAb only, and control IgG-DOTA-PRIT). It was determined that the clinical morbidity in 3/3 (100%) animals was apparently due to adverse effects of estrogen treatment (see Table S7).

Hematology, clinical chemistry, and histopathology

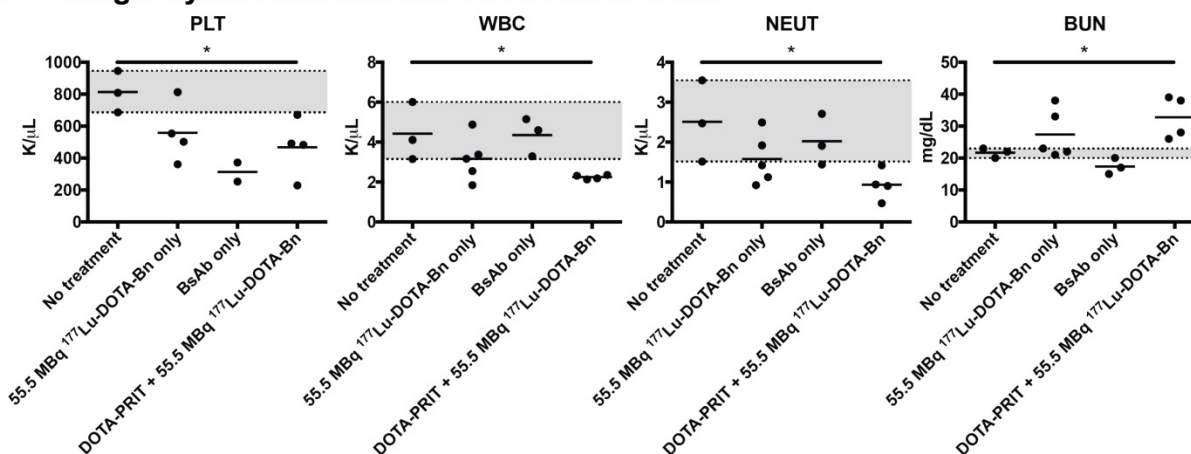
Small tumors, single cycle: At ~85 d following treatment of mice bearing small-sized s.c. tumors with a single cycle of anti-HER2-DOTA-PRIT + 55.5 MBq ^{177}Lu -DOTA-Bn, of the five animals with CRs submitted for necropsy (a single mouse from BsAb only and four from the anti-HER2-DOTA-PRIT treatment groups), four were cured—one from the BsAb only group (1/3, 33.3%) and three from the anti-HER2-DOTA-PRIT treated group (3/4, 75%). No remarkable treatment-related morphological change

was noted (Table S8). Hematology and clinical chemistry values were within normal ranges with the exception of white blood cell (WBC), platelet (PLT), and neutrophil (NEUT) values, which were significantly lower ($P = 0.014$, 0.020 , and 0.017 , respectively) in the anti-HER2-DOTA-PRIT treated group ($n = 4$; WBC range: 2.13-2.36 K/ μ L; PLT range: 229-670 K/ μ L; NEUT range: 0.47-1.42 K/ μ L) compared to the non-treated group ($n = 3$; WBC range: 3.15-6.01 K/ μ L; PLT range: 686-946 K/ μ L; NEUT range: 1.51-2.47 K/ μ L) (Figure 9, Figure S8 and Figure S9). Also, blood urea nitrogen (BUN) was significantly elevated ($P = 0.020$) in the anti-HER2-DOTA-PRIT-treated group ($n = 4$; BUN range: 26.0-39.0 mg/dL) compared to the non-treated group ($n = 3$; BUN range: 20.0-23.0 mg/dL), suggesting impaired renal function. Creatinine (CREA) was also elevated in the anti-HER2-DOTA-PRIT-treated group ($n = 4$; CREA

range: 0.21-0.36 mg/dL) compared with the non-treated group ($n = 3$; CREA range: 0.20-0.21 mg/dL), although the difference was not significant ($P = 0.062$).

Medium tumors, single cycle: At ~200 d following treatment of mice bearing medium-sized s.c. tumors with anti-HER2-DOTA-PRIT + 11.1-55.5 MBq ^{177}Lu -DOTA-Bn, there were a total of six survivors, including two CRs, one from each of the 11.1 MBq and 55.5 MBq groups. Both were determined to be cured. No remarkable treatment-related histopathology was noted (Table S9). Hematology and clinical chemistry values were within normal ranges (Figures S10 and Figure S11). Due to the absence of surviving non-treated controls and the small number of survivors of animals treated with anti-HER2-DOTA-PRIT at ~200 d, statistical comparisons for hematology and clinical chemistry parameters were not conducted for this study.

A Single-cycle treatment anti-HER2-DOTA-PRIT



B Fractionated 3-cycle treatment anti-HER2-DOTA-PRIT

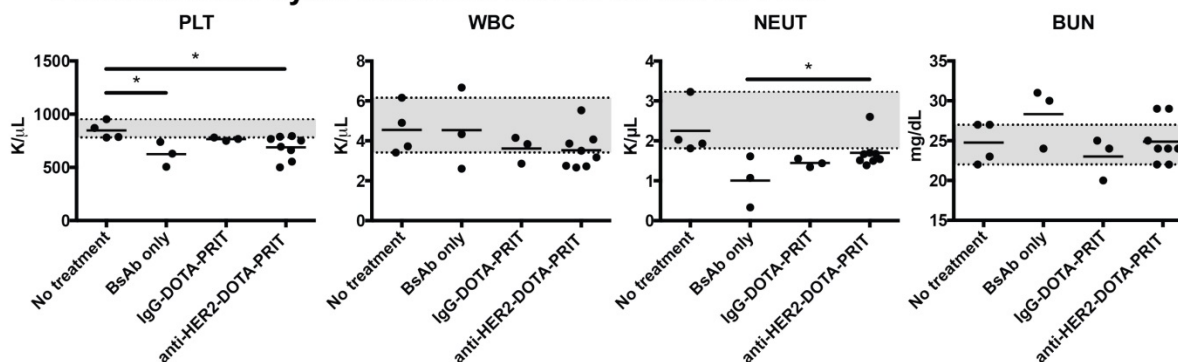


Figure 9. Hematology and clinical chemistry observed at 85 d following treatment with either (A) single cycle of anti-HER2-DOTA-PRIT + 55.5 MBq of ^{177}Lu -DOTA-Bn (total activity: 55.5 MBq/mouse) or (B) fractionated three-cycle treatment of anti-HER2-DOTA-PRIT + 55.5 MBq of ^{177}Lu -DOTA-Bn (total activity: 167 MBq/mouse). The range of values for the animals given no treatment is shaded in grey for reference.

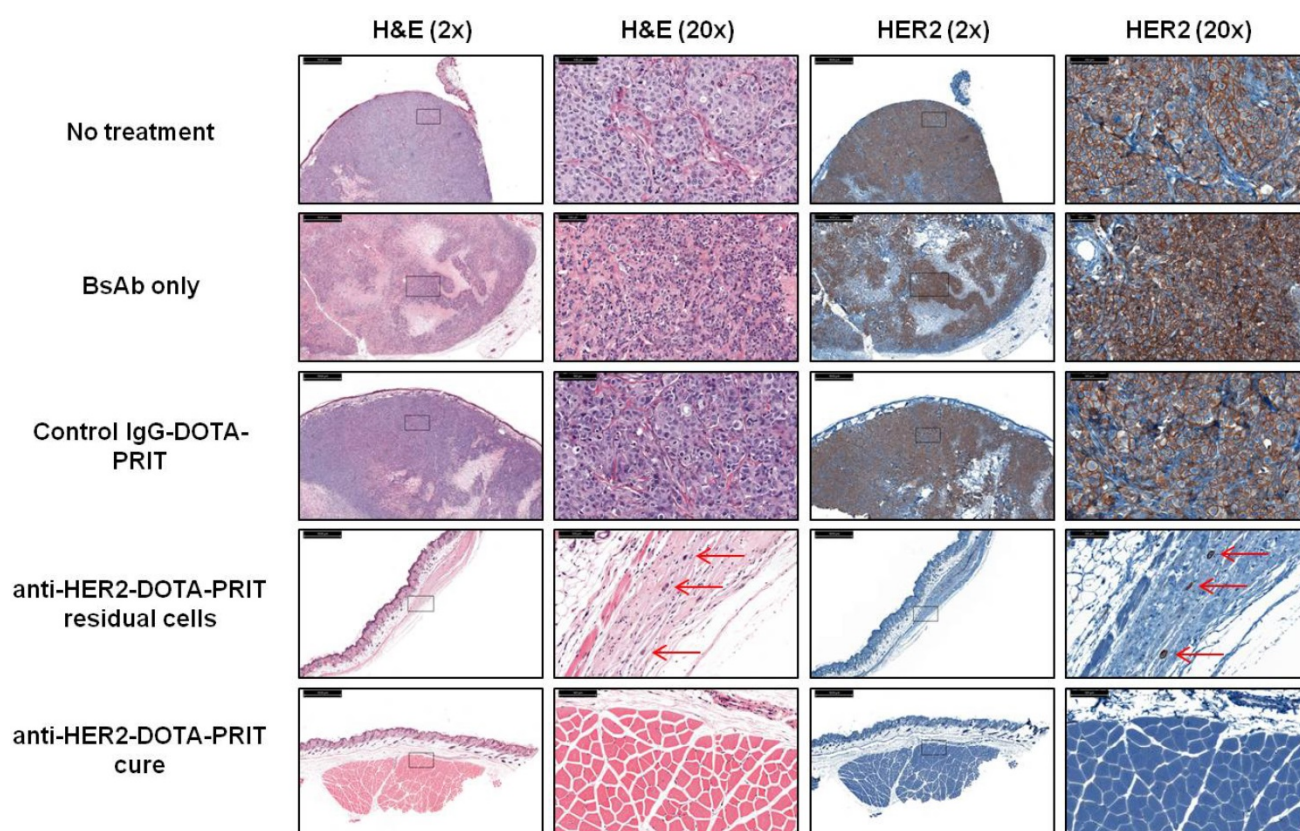


Figure 10. Morphologic analysis of the site of BT-474 tumor inoculation at 85 d shows that treatment with anti-HER2-DOTA-PRIT leads to cures (5/8) or microscopic residual disease (red arrows; 3/8), while controls (10/10) show bulk tumor present by H&E staining (please see **Table S8** for detailed description). IHC analysis shows that all residual tumors are HER2 antigen positive.

Medium tumors, three cycles: For the fractionated treatment study, a high frequency of cures was seen with anti-HER2-DOTA-PRIT (5/8, 62.5%) at 85 d post-treatment. The other three treated animals (3/8, 37.5%) showed microscopic residual disease, primarily consisting of soft tissue sclerosis with a few scattered neoplastic cells (**Table S10**). Representative H&E staining of tissue sections taken from the site of tumor inoculation for all treatment groups is shown in **Figure 10**.

Also at 85 d post-treatment, two anti-HER2-DOTA-PRIT animals (2/8) showed hematology and clinical chemistry values that were out of range, while no changes were observed in 6/8 animals (**Figure 9**, **Figure S12** and **Figure S13**). Low severity histopathologic changes in the bone marrow were limited to only 1 animal for the anti-HER2-DOTA-PRIT-treated group (1/8, 12.5%; severity score: 1; **Table S11**). A single mouse exhibited mild anemia (7.70 M/ μ L; control range: 8.38-8.88 M/ μ L) and hypohemoglobinemia (HGB; 12.7 g/dL; control range: 14.3-14.7 g/dL) as well as increases of aspartate aminotransferase (154 U/L; control range: 57-81 U/L) and alanine phosphatase (128 U/L; control range: 64-110 U/L). Another mouse showed mild anemia (7.89 M/ μ L), HGB (13.1 g/dL), and

thrombocytopenia (500 K/ μ L; control range: 781-953 K/ μ L), but normal clinical chemistry values. In summary, a few hematology parameters had values significantly different from physiologic ranges in the anti-HER2-DOTA-PRIT group versus no treatment group, while no significant differences were seen for clinical chemistry. Anemia and thrombocytopenia were significant ($P < 0.05$) in the anti-HER2-DOTA-PRIT-treated group ($n = 8$; RBC range: 7.70-8.63 M/ μ L; PLT range: 500-794 K/ μ L) compared to the non-treated group ($n = 4$; RBC range: 8.38-8.88 M/ μ L; PLT range: 781-953 K/ μ L).

Discussion

We have optimized DOTA-PRIT to permit targeting of massive amounts of radiation to tumor, while sparing normal tissue. Anti-HER2-DOTA-PRIT + ^{177}Lu -DOTA-Bn can inhibit growth of HER2(+) BT-474 breast cancer xenografts and improve survival without causing significant morphologic changes in normal target tissues when assessed at 85-200 d after treatment. On the other hand, our preliminary assay of toxicity revealed some individual variation of some hematological and hematochemical parameters with discrepancy to the dosimetry and histopathology. Overall, a functional impairment assessed through

measurement of specific blood values might not necessarily mirror or imply an anatomic damage. In general, for many organ systems (e.g., liver, kidney), functional or sublethal damage and its severity often do not always correlate with an anatomic lesion, nor with morphologic severity, as the sensitivity and specificity can differ in terms of methods and parameters (please see ref. [20]). In some cases, the discrepancy might be due to a temporal factor, as leakage of cytoplasmic enzymes in the blood stream, for instance, might precede a structural breakdown of a cell. Another reason may be due to the often limited correlation between CBC values and the bone marrow histopathologic evaluation, as the latter tends to be less sensitive and can also vary depending on the body region and the different distribution of the myeloid and erythroid elements inside the marrow cavity.

Since all groups received estrogen supplementation, hematologic changes are likely due to anti-HER2-DOTA-PRIT + ^{177}Lu -DOTA-Bn alone or to synergy between the two test items and estrogen. Paradoxically, abnormal hematologic and clinical chemistry values (low PLT, WBC, and NEUT, as well as elevated BUN) were observed at high incidence (4/4, 100%) in the group treated with a single cycle of anti-HER2-DOTA-PRIT + ^{177}Lu -DOTA-Bn (total 55.5 MBq/mouse), while only a few animals (2/8, 25%) receiving fractionated treatment (total 167 MBq/mouse) showed significant out-of-value ranges. In order to address all of the above open questions, more comprehensive toxicity experiments with larger numbers of animals per group will be performed to examine the effects of dose, as well as to evaluate changes at multiple time-points following treatment to determine if any changes and toxicity are acute only or chronic.

HER2 (transmembrane tyrosine kinase receptor HER2/neu or c-erbB-2; molecular weight: 185 kD) is a member of the HER/erbB family of cell surface receptors widely expressed on common solid tumors of humans, including breast [21], gastric [22], and gynecologic malignancies [23]. Trastuzumab, an anti-HER2 antibody, can prolong survival in patients with HER2(+) breast or ovarian cancer [24, 25]. Unfortunately, despite initial response to trastuzumab, resistance is common [26]. To enhance the efficacy of trastuzumab, antibody-based delivery of a cytotoxin [27] or therapeutic radionuclide [28] has been tested. Several preclinical RIT studies with trastuzumab-radioisotope conjugates have also been described (e.g., with α -emitters or β -emitters); however, as with other conventional RIT strategies, the TI could potentially be improved with a PRIT approach.

Although herein we do not conduct a comparison with conventional anti-HER2 ^{177}Lu -RIT with an IgG radiolabeled with ^{177}Lu , it was previously reported by Rasaneh et al. [29] with 8- to 10-week-old inbred female BALB/c mice that the calculated mean absorbed doses to tumor and blood during treatment with 7.4 MBq were $6.35 \pm 1.2 \text{ Gy MBq}^{-1}$ and $1.62 \pm 0.13 \text{ Gy MBq}^{-1}$, leading to a mean TI for blood of 3.9. During a comparative study of ^{227}Th -labeled and ^{177}Lu -labeled trastuzumab in mice bearing HER2(+) SKOV-3 ovarian cancer xenografts, absorbed radiation doses from β -particles emitted from ^{177}Lu in the tumor and blood were $3.82 \pm 0.64 \text{ Gy}$ and $1.57 \pm 0.64 \text{ Gy}$ for 72 MBq/kg ^{177}Lu -trastuzumab injection, giving an approximate mean TI of 2.4 for blood [30]. In addition, although dosimetry was not described, Ray et al. reported that i.p. administration of 18.5-27.75 MBq ^{177}Lu -trastuzumab into 4- to 6-week-old female athymic mice (nu/nu) bearing HER2-expressing human colorectal xenografts was associated with myelotoxicity and loss of therapeutic benefit, suggesting that the low TI for blood was responsible [31]. Perhaps our effective therapeutic regimen is comparable to what was chosen for the treatment of s.c. ovarian cancer xenografts with a ^{177}Lu -labeled anti-HER2 nanobody (^{177}Lu -DTPA-2Rs15d; MW < 15 kDa). Impressively, D'Huyvetter et al. [32] reported a TI for blood of 900 with ^{177}Lu -DTPA-2Rs15d nanobody co-infused with 150 mg/kg Gelofusin (^{177}Lu -nanobody + Gelofusin), compared with a TI for blood of 1.32 for ^{177}Lu -trastuzumab. This high TI for blood was further supported by the fact that the authors could treat tumor-bearing female athymic nude mice ($20 \pm 5 \text{ g}$ body weight) with 7 i.v. injections (once a week, over a period of seven weeks) with $\sim 21 \text{ MBq}$ of ^{177}Lu -nanobody + Gelofusin (total $\sim 147 \text{ MBq}$ /mouse; total estimated absorbed tumor dose based on tumor dosimetry of 0.9 Gy/MBq : $\sim 132 \text{ Gy}$) without apparent toxicity. A notable drawback of nanobody-based targeted radionuclide therapy is the low TI for kidney of 1, even with reduction of kidney accumulation using Gelofusin co-infusion.

Prior to this study, we have reported DOTA-PRIT for GD2- [7] and GPA33-expressing human xenograft tumors [8, 33] in laboratory animals, and have developed effective treatment regimens capable of achieving 100% CRs and a high probability of histologic cures with limited toxicity. We observed TIs of 142 for blood and 23 for kidney with 84.9 cGy/MBq to GD2(+) tumors, and TIs of 73 for blood and 12 for kidney with 65.8 cGy/MBq to GPA33(+) tumors. These two target systems have potential clinical utility for a variety of human solid tumors, including colon cancer, pancreatic cancer,

pseudomyxoma peritonei, and subsets of pancreatic cancer for GPA33, as well as for neuroblastoma, glioma, sarcoma, and small cell lung cancer for GD2. In contrast to GPA33 and GD2, the HER2 system is thought to be much more labile in the membrane as well as more rapidly internalized once bound to its cognate antibody, so the HER2 target is challenging for successful anti-tumor therapy with DOTA-PRIT. To study this issue, we prepared anti-HER2-C825 product with sufficient affinity, biochemical purity, and yields for *in vivo* studies. We sought an animal model system for comparison of DOTA-PRIT treatment response, and we chose the human BT-474 breast cancer cell line, a very high HER2-expressing tumor. We chose this model in part because it was reported that the level of HER2 expression is a predictor of antibody-HER2 trafficking behavior in cancer cells, and that HER2-overexpressing cells (such as SK-BR-3, BT-474, HCC1419, and HCC1954) display a high level of antibody persistence on their plasma membrane due to a combination of efficient HER2 recycling and limited reduction in HER2 levels upon antibody treatment [34]. In addition, preclinical therapeutic anti-HER2 pretargeting has been previously reported in BT-474 xenografts [35-37], although not with radioisotopes.

The most direct treatment regimen for comparison with the other two DOTA-PRIT solid tumor systems was triple-cycle fractionated regimen of medium-sized tumors, in the range of 100-400 mg size. We chose a triple-cycle approach, which was also used for GPA33 and GD2 targeting, because we reasoned that a fractionated treatment approach would be ideal for safe administration of sufficient ^{177}Lu -DOTA-Bn activity to achieve a tumoricidal absorbed radiation dose to tumor of ~ 70 Gy [1]. We demonstrated HER2(+) BT-474 tumor growth control, including cures with optimized dosing. We found that triple-cycle fractionated anti-HER2-DOTA-PRIT (total IA: 167 MBq/mouse) was well tolerated and highly effective, with no animals showing acute toxicity. The total dose of radiation to tumor was ~ 70 Gy, with a high frequency of CRs (8/8, 100%), complete tumor eradication to cure (5/8, 62.5%), and 37.5% microscopic residual disease (3/8) at 85 d. No CRs recurred within 85 d. We verified using serial SPECT/CT imaging that efficient tumor targeting was achieved during each treatment cycle. Survivors in control groups showed tumor progression $207 \pm 201\%$ of pre-treatment volume at approximately 85 d, with no CRs or cures.

In terms of tumor response, we observed a size-dependent effect during efficacy studies, with smaller-sized tumors requiring only a single cycle of anti-HER2-DOTA-PRIT + 55.5 MBq of ^{177}Lu -DOTA-

Bn to achieve a high incidence of regression to CRs (5/5, 100%) and cures (3/4, 75%; at 85 d). The observation that complete remission was possible in these animals with such a relatively low estimated absorbed dose to tumor of 22 Gy was likely due in part to the effect of the trastuzumab-like action of the BsAb (1.19 nmol administered/mouse). Single-dose treatment of medium-sized tumors, however, resulted in a low frequency of CRs (2/15, 26.7%) or cures (2/6 assessable animals at 200 d), irrespective of administered ^{177}Lu -DOTA-Bn (11.1-55.5 MBq). In addition, in a single mouse bearing a medium-sized tumor (pretreatment volume: 155 mm³), a single dose of 33.3 MBq led to significant tumor regression to a minimum volume of 13 mm³ at ~ 100 days post-treatment, but then recurred to 170 mm³ at 200 d, suggesting that tumor regrowth was likely in undertreated tumors. As described above, triple-cycle treatment of 55.5 MBq was highly effective for the medium-sized tumors, leading to a high frequency of CRs and cures.

For anti-HER2-DOTA-PRIT, we implemented a theranostic isotope to permit simultaneous therapy and imaging. ^{177}Lu has a physical half-life of 6.73 days (d), and is an emitter of both β -particles and γ -radiation (β -maximum energy: 0.5 MeV; β -particle range in tissue R_{max} : 2 mm; γ : 208 keV, 11% abundance), allowing for therapy and γ -scintigraphy, respectively. We have focused our efforts on ^{177}Lu for DOTA-PRIT treatment of solid tumors, since the long biological retention kinetics of pretargeted ^{177}Lu -DOTA-Bn in tumor for GD2 and GPA33 is a good match with the long physical half-life of ^{177}Lu , and its relatively short β -particle range is theoretically well-suited for treatment of smaller tumor volumes (optimal tumor diameter for cure probability of 0.9 = 2.0 mm [38]) while minimizing collateral radiation damage to normal tissues. Finally, the ^{177}Lu γ -emissions allow for high-resolution SPECT/CT imaging for pre-therapy dosimetry as well as treatment monitoring, which is emerging as a quantitative clinical imaging modality for targeted therapies with ^{177}Lu radiopharmaceuticals [39, 40].

We acknowledge that comparable PRIT studies exist in the literature with internalizing targets, but as far as we are aware, this study represents the first report of curative and safe multistep PRIT with an internalizing antigen as the target. We observed TIs of 28 for blood and 7 for kidney with 39.9 cGy/MBq to HER2(+) tumors. Although direct comparison with TI is not possible because TIs were not calculated, Sharkey et al. [41] successfully adapted an anti-hapten PRIT strategy using the internalizing antibody-antigen system anti-Trop-2 antibody RS7-Trop-2, showing mean tumor-to-blood ratios of 1037, 378, and

62 at 3 hours post-injection of ^{111}In -haptin in MDA-MD-468, SK-OV-3, and PC3 models, respectively. Subsequent fractionated therapy studies by van Rij et al. [42] with a dose of $3 \times 41 \text{ MBq } ^{177}\text{Lu}$ -haptin/cycle in a PC3 model showed improved median survival at the expense of hematological toxicity; however, conventional RIT with the parent mAb ^{177}Lu -hRS7 (11 MBq) was at least as effective with similar toxicity, likely due to the large difference in tumor uptake between ^{177}Lu -hRS7 (62 %ID/g) and TF12/ ^{177}Lu -haptin (8.0-9.2 %ID/g). Alternatively, *in vivo* efficacy using a bioorthogonal click PRIT approach to tumor targeting was demonstrated by Houghton et al. [43] with the internalizing anti-CA19.9 antibody 5B1-CA19.9, reporting a TI for blood of 11.4 in a BxPC3 model.

The translational feasibility of this approach must be determined empirically, and will require detailed clinical studies including dose response with ^{177}Lu and careful theranostic dose assessment for individual patients. During BsAb-pretargeting, the doses are highly dependent on the BsAb concentration localized on the tumor. As described in previous clinical studies with BsAb pretargeting (e.g., please see refs. [44-47]), we anticipate using pretherapeutic scouting/imaging for patient-tailored dosimetry, followed with higher doses for therapy, likely in the same range as peptide receptor radionuclide therapy (e.g., during initial human studies with ^{177}Lu -DOTA-JR11 for somatostatin receptor targeting: 3 cycles (total 15.2 GBq) to achieve tumor doses up to 487 Gy in patients with metastasized neuroendocrine neoplasias (grades G1-G3)) [48].

In summary, the present research shows proof of principle for the development of a high-TI theranostic approach for PRIT of HER2(+) disease. Curative therapies for HER2-expressing tumors are a major unmet need. Treatment options are limited for patients with HER2-overexpressing cancers, especially those resistant to trastuzumab and kinase inhibitors [49]. We consider this success of anti-HER2-DOTA-PRIT as a benchmark for comparison to other internalizing antigen targets.

Methods

Cloning and expression of anti-HER2-C825 BsAb

HER2-C825 BsAb was prepared as an IgG-scFv [12] format using the sequences for trastuzumab [50] and C825 [11]. It was made using the exact same platform as hu3F8-C825 [7], only replacing variable regions (VH and VL) of hu3F8 with those of trastuzumab. The BsAb (molecular weight: ~210 kDa)

was produced in CHO cells and purified by protein A affinity chromatography as previously described [7]. The control BsAb huA33-C825 was made using the same platform as previously described [8]. Biochemical purity analysis of the BsAb was performed using SE-HPLC (column: TSKgel G3000SWxl; running buffer: 400 mM sodium perchlorate pH 6.0; flow rate 0.5 mL/min), with eluted BsAb detected by UV absorbance at 280 nm.

Surface plasmon resonance studies

The Biacore T100 Biosensor, CM5 sensor chip, and related reagents were purchased from GE Healthcare. A BSA-(Y)-DOTA-Bn conjugate was prepared as previously described [7]. The antigen was immobilized using the Amine Coupling Kit (GE Healthcare). Purified BsAbs were analyzed, and data were fit to a bivalent analyte model using the Biacore T100 evaluation software as previously described [7].

Cell lines

BT-474 is ductal carcinoma with epithelial morphology, luminal B subtype, estrogen receptor α -positive [ER(+)], progesterone-positive/-negative [PR(+/-)] and HER2-positive [HER2(+)], while MDA-MB-231 is adenocarcinoma with epithelial morphology, claudin-low subtype, and a triple-negative immunoprofile (ER(-), PR(-), and HER2(-)) [43]. Cell lines were obtained from American Type Culture Collection (Manassas, VA) and periodically tested for mycoplasma negativity using a commercial kit (Lonza). All cell lines were maintained in a humidified incubator containing 5% CO_2 at 37 °C, limited to fewer than 10 passages, and cultured in Dulbecco's modified Eagle-high-glucose/F-12 (DME-HG/F-12) medium supplemented with non-essential amino acids (0.1 mM), 10% heat-inactivated fetal calf serum (FCS), 100 units/mL of penicillin, and 100 $\mu\text{g}/\text{mL}$ streptomycin.

Internalization and cellular processing of anti-HER2-C825

Trastuzumab is known to internalize upon binding to surface HER2 antigen [15]. The internalization kinetics of anti-HER2-C825 following binding to BT-474 cell surface HER2 antigen at 37 °C were assessed using the radiotracer ^{131}I -anti-HER2-C825 based on previously described assays [51, 52]. In brief, cells were plated at a density of 5.0×10^5 cells/mL in 12-well plates and allowed to adhere overnight. Cells were pre-incubated on ice with ^{131}I -anti-HER2-C825 (prepared using the IODOGEN method [53] to a specific activity of 132 MBq/mg and purified using SEC to radiochemical purity >98% and diluted into complete media; 160 ng/mL; 0.8 nM) for 1 h. Next, the cells were extensively washed with

complete media chilled on ice and the plates were transferred to the 37 °C incubator. At various time-points up to 24 h, the radioactive distribution in the outside media, cell surface, as well as the fraction of activity internalized by the cells was determined ($n = 3-6$ per time-point) by quantification in the gamma counter. An acid wash protocol was used to strip cell-surface antibody, consisting of treating the cells on ice three times for 5 min with 2 M urea, 50 mM glycine, 150 mM NaCl, pH 2.4, and pooling the supernatants. The outside media was assayed further using trichloroacetic acid (TCA) precipitation (~1 mL of collected media was mixed with 0.9 mL of 20% w/v TCA) to determine if the ^{131}I activity was antibody-bound (suggesting passive dissociation or “shedding” [52]), or in the form of low-molecular-weight metabolites, suggesting intracellular metabolism followed by exocytosis. Controls consisted of either incubation at 4 °C or wells consisting of the ^{131}I -anti-HER2-C825 diluted into media only. These control wells were also subjected to TCA precipitation in order to inhibit internalization and determine the basal catabolism (via degradation) rate of the tracer, respectively. For kinetic analysis, data was curve-fitted using a nonlinear model, with one-phase association using Prism software package, Graphpad Software Inc., San Diego, CA.

Xenograft models

All animal experiments were approved by the Institutional Animal Care and Use Committee of Memorial Sloan Kettering Cancer Center (New York, NY), and institutional guidelines for the proper and humane use of animals in research were followed. Female athymic nude mice (nu/nu, 6-8 weeks old) were obtained from Harlan/Envigo. Mice were allowed to acclimate for a minimum of one week. For the BT-474 tumor model, mice were implanted with estrogen (17 β -estradiol; 0.72 mg/pellet 60-d release; Innovative Research of America) by trochar injection 3 d before inoculation with cells. No estrogen supplementation was required for the MDA-MB-231 xenograft model. For establishment of all tumor xenografts, mice were inoculated with 5.0×10^6 cells in a 200 μL cell suspension of a 1:1 mixture of media with reconstituted basement membrane (BD Matrigel™, Collaborative Biomedical Products Inc., Bedford, MA) on lower flank via s.c. injection, and used within 3-4 weeks. Tumor volumes were estimated using the formula for the volume (V) of an ellipsoid: $V = 4/3\pi(\text{length}/2 \times \text{width}/2 \times \text{height}/2)$, with dimensions in mm.

Anti-HER2-DOTA-PRIT reagents and dosing protocol

The three anti-HER2-DOTA-PRIT reagents were anti-HER2-C825 BsAb, CA, and ^{177}Lu -DOTA-Bn. All reagents were administered intravenously (i.v.) via a lateral tail vein and given at the following times relative to ^{177}Lu -DOTA-Bn injection: $t = -28$ h for anti-HER2-C825, followed by CA at $t = -4$ h and ^{177}Lu -DOTA-Bn at $t = 0$ h. The CA (a 500 kDa dextran-(Y)-DOTA-Bn conjugate; 61 mol of (Y)-DOTA-Bn per mole of dextran) was prepared according to previously described methods [14] and formulated in saline for injection. ^{177}Lu -DOTA-Bn was also prepared according to previously described methods [8]. Radioactivity in samples was measured using a CRC-15R dose calibrator (Capintec, Ramsey, NJ) using the appropriate settings for each isotope.

Biodistribution studies to optimize *in vivo* anti-HER2-DOTA-PRIT

Prior to therapy studies, BsAb and CA dose-titration experiments were carried out in groups of BT-474 tumor-bearing mice with tracer administered activities of ^{177}Lu -DOTA-Bn/mouse (5.6 MBq (~30 pmol)) to optimize DOTA-PRIT reagent doses for efficient *in vivo* tumor targeting. For this purpose, we had specific TI benchmarks of at least 20:1 for blood and 10:1 for kidney at 24 h p.i. of ^{177}Lu -DOTA-Bn, while maximizing radioactivity uptake in tumor. Groups were sacrificed at 24 h p.i. of ^{177}Lu -DOTA-Bn for biodistribution assay of ^{177}Lu activity in select tissues. For biodistribution analysis, mice were euthanized by $\text{CO}_2(\text{g})$ asphyxiation, and tumor and selected organs were harvested, rinsed with water and allowed to air-dry, weighed, and radioassayed by gamma scintillation counter (PerkinElmer Wallac Wizard 3”). Count rates were background- and decay-corrected, converted to activities using a system calibration factor specific for the isotope, normalized to the administered activity, and expressed as %IA/g (mean \pm SEM).

Dosimetry calculations

For dosimetry calculations, a serial biodistribution study was carried out in BT-474 tumor-bearing mice ($n = 24$) with the optimized DOTA-PRIT protocol + 5.5-6.1 MBq (~30 pmol) of ^{177}Lu -DOTA-Bn. Groups of HER2(+) BT-474 tumor-bearing mice ($n = 4-5$) were given PRIT + 5.5-6.1 MBq (~30 pmol) of ^{177}Lu -DOTA-Bn and sacrificed at 1.0 ($n = 5$), 2.5 ($n = 5$), 24 ($n = 5$), 96 ($n = 5$), and 336 h p.i. ($n = 4$) for biodistribution analysis of ^{177}Lu activity in tumor and selected normal tissues (please see **Table S2** for tissue activity concentration data). For each tissue, the non-decay-corrected

time-activity concentration data were fit using Excel to a 1-component, 2-component, or more complex exponential function as appropriate, and analytically integrated to yield the cumulated activity concentration per unit administered activity (MBq-h/g per MBq). The ^{177}Lu equilibrium dose constant for non-penetrating radiations (8.49 g-cGy/MBq-h) was used to estimate the tumor-to-tumor and select organ-to-organ self-absorbed doses, assuming complete local absorption of the ^{177}Lu beta rays only, and ignoring the gamma ray and non-self dose contributions.

Immunohistochemical (IHC) and autoradiography experiments

For IHC of HER2-expressing tumors, groups of BT-474 tumor-bearing nude mice were administered i.v. 0.25 mg (1.19 nmol) of anti-HER2-C825. At 24 h p.i., the animals were sacrificed and tumors were frozen in OCT. IHC detection of HER2 was performed by the Molecular Cytology Core Facility of Memorial Sloan Kettering Cancer Center using Discovery XT processor (Ventana Medical Systems). The tissue sections were blocked for 30 min in 10% normal goat serum and 2% BSA in PBS. Next, the sections were incubated with a rabbit polyclonal HER2 antibody (Enzo, cat# alx-810-227) at 5.0 $\mu\text{g}/\text{mL}$ concentrations for 5 h, followed by 1 h incubation with biotinylated goat anti-rabbit IgG (Vector Labs, cat# PK6101) at 5.75 $\mu\text{g}/\text{mL}$. The detection was performed with Blocker D, Streptavidin-HRP, and DAB detection kit (Ventana Medical Systems). All reagents were used according to the manufacturer's instructions. For IHC to determine anti-HER2-C825 antibody distribution, the same procedure was followed except the primary antibody step was excluded and biotinylated goat anti-human IgG (Vector Labs, cat# BA3000) antibody was used.

For *ex vivo* autoradiography, tumors were excised, snap-frozen, and embedded in OCT at 24 h p.i. of ^{177}Lu -DOTA-Bn. Series of sequential 10 μm thick cryosections were cut immediately and exposed to a phosphor plate overnight at $-20\text{ }^\circ\text{C}$ for determination of ^{177}Lu activity distribution. Digital autoradiographic images at 25 μm pixel size were obtained as follows: tumor sections were exposed to a phosphor-imaging plate (Fujifilm BAS-MS2325, Fuji Photo Film, Japan) overnight at $-20\text{ }^\circ\text{C}$. Upon completion of the exposure, the imaging plates were removed from the cassette and placed in a Typhoon FLA 7000 (GE Healthcare, USA) to read out the image. The image reader creates 16-bit grayscale digital images with a pixel size of 25 μm , which are then converted to tiff image format files for subsequent analysis. Finally, H&E staining was performed to

visualize tumor morphology in consecutive sections, and images were acquired in a similar manner. Images were manually registered using Photoshop CS6 software (Adobe Systems).

Theranostic anti-HER2-DOTA-PRIT therapy

To evaluate the toxicity and efficacy of anti-HER2-DOTA-PRIT therapy in an animal model of human breast cancer, therapy studies were carried out in BT-474 tumor-bearing mice with either small or medium-sized s.c. xenografts. Tumors with volumes ranging from palpable to 30 mm^3 were classified as small, and those ranging from 100-400 mm^3 were classified as medium-sized. Treatment groups were monitored for 85-200 d and survivors were submitted for histopathology studies (*vide infra*).

Initially, single-cycle treatment with anti-HER2-DOTA-PRIT + 55.5 MBq of ^{177}Lu -DOTA-Bn (300 pmol) was evaluated in groups of mice bearing small s.c. xenografts and compared with treatment controls (estimated dose to tumor: 22 Gy). These groups were monitored for 85 d post-treatment. During this study, planar scintigraphy (using previously described methods [7]) was used up to 70 h p.i. of ^{177}Lu -DOTA-Bn to verify tumor targeting of ^{177}Lu activity.

Next, groups of mice bearing medium-sized s.c. xenografts were treated in a single-cycle anti-HER2-DOTA-PRIT dose escalation trial with 11.1, 33.3, or 55.5 MBq of ^{177}Lu -DOTA-Bn (60-300 pmol)/mouse and compared with control groups (estimated absorbed radiation doses to tumor: 4.4-22 Gy). These groups were monitored for \sim 200 d post-treatment in order to study tumor recurrence and chronic toxicity of anti-HER2-DOTA-PRIT.

In a third therapeutic study, a three-cycle fractionated DOTA-PRIT regimen with 55.5 MBq of ^{177}Lu -DOTA-Bn (300 pmol)/mouse/cycle was evaluated in groups of mice bearing medium-sized s.c. xenografts (estimated absorbed radiation doses to tumor: 70 Gy). To achieve this, the total IA of 167 MBq ^{177}Lu -DOTA-Bn/mouse was given in three equal weekly administrations, with each of the three DOTA-PRIT reagents given during each cycle (designated as "anti-HER2-DOTA-PRIT"). A control treatment arm was included that replaced anti-HER2-C825 with the anti-GPA33 targeting BsAb huA33-C825 [8] (designated as "control IgG-DOTA-PRIT") in order to verify that efficacy was dependent on anti-HER2-C825 tumor-specific targeting. These groups were monitored for \sim 85 d post-treatment. Three mice undergoing treatment with anti-HER2-DOTA-PRIT, as well as a single mouse undergoing control IgG-DOTA-PRIT, were randomly selected for SPECT/CT imaging using previously

described methods [33] to assay tumor targeting and quantify tumor uptake of ^{177}Lu activity. Notably, the whole animal was not imaged because of the length of time required for each scan (30–40 min per mouse); the imaging field-of-view was limited to the caudal half of the animal (midline to tail).

Response to therapy and toxicity assessment

Mice were monitored daily and weighed at least twice weekly for evidence of treatment-induced toxicity. Animals were observed until they were sacrificed due to excessive tumor burden $>2500\text{ mm}^3$ or less if tumor caused mobility concerns. Animals showing a weight loss of greater than 15% of their initial (pre-treatment) body weight in 1 or 2 d, or 20% or more of their pre-treatment weight, were removed from the group at that time and sacrificed. To further evaluate toxicity, randomly selected animals undergoing treatment were submitted for histopathologic evaluation of the xenotransplant, kidney, bone marrow (sternum, vertebrae, femur, and tibia), liver, and spleen (unless otherwise noted) by a board-certified veterinary pathologist at Memorial Sloan Kettering Cancer Center's Laboratory of Comparative Pathology. Hematology and clinical chemistry panels were also collected. A CR is defined as tumor regression to a tumor volume equal to or smaller than 4.2 mm^3 , and a cure is defined as no histopathologic evidence of neoplasia at the site of tumor inoculation at necropsy. Tumor measurements were considered accurate to a diameter of $2\text{ mm} \times 2\text{ mm} \times 2\text{ mm}$, which led to a calculated volume (assuming ellipsoidal geometry as described above) of 4.2 mm^3 ; anything smaller was designated as "palpable" until the tumor completely disappeared. The breast cancer xenografts developed distant metastasis in 33.3% (2/6) of treated survivors at 200 d, but in no animals evaluated at 85 d (Tables S7–S9).

Statistics

All statistics were determined using the Prism software package, Graphpad Software Inc., San Diego, CA. Statistical comparisons between two individual groups were analyzed by student's unpaired *t*-test when appropriate, with the level of statistical significance set at $P < 0.05$. Survival curves were compared using Log-rank (Mantel-Cox) test.

Acknowledgments

We would like to thank Ms. Valerie Longo and Dr. Sean Carlin for assistance with animal imaging and immunohistochemistry/autoradiography experiments, respectively. We would also like to thank comparative pathologist Dr. Sebastien Monette for his contribution to the review and interpretation of histopathology, hematology, and clinical chemistry.

This study was supported in part by the Donna & Benjamin M. Rosen Chair (to S.M. Larson), Enid A. Haupt Chair (to N.K. Cheung), The Center for Targeted Radioimmunotherapy and Theranostics, Ludwig Center for Cancer Immunotherapy of Memorial Sloan Kettering (MSK) Cancer Center (to S.M. Larson), and Mr. William H. Goodwin and Mrs. Alice Goodwin and the Commonwealth Foundation for Cancer Research and The Experimental Therapeutics Center of MSK (to S.M. Larson). S.M. Larson was also supported in part by NIH grant P50 CA86438. We also acknowledge the NIH/NCI Cancer Center Support Grant (P30 CA08748) for use of the Tri-Institutional Laboratory of Comparative Pathology, MSK Cancer Center, Weill Cornell Medicine, and The Rockefeller University, New York, NY. Technical services provided by the MSK Small-Animal Imaging Core Facility were also supported by P30 CA08748. A Shared Resources Grant from the MSK Cancer Center Metastasis Research Center (to P. B. Zanzonico), which provided funding for the purchase of the NanoSPECT/CT Plus, is gratefully acknowledged. We are also grateful to Ms. Leah Bassity for her editorial assistance.

Abbreviations

BsAb: bispecific antibody; BUN: blood urea nitrogen; CA: clearing agent CR: complete responses; CREA: creatinine; HGB: hemoglobin; IHC: immunohistochemistry; IA: injected activity; i.v.: intravenous; %IA/g: percent injected activity per gram; PLT: platelets; p.i.: post-injection; PRIT: pretargeted radioimmunotherapy; RIT: radioimmunotherapy; [M]-DOTA-Bn: radiometal complex of S-2-(4-aminobenzyl)-1,4,7,10-tetraazacyclododecane tetraacetic acid chelate; RBC: red blood cells; ROI: region-of-interest; SPECT/CT: single-photon emission computed tomography/computed tomography; SEM: standard error of the mean; s.c.: subcutaneous; TI: therapeutic index; tumor-to-blood ratio: T/B, tumor-to-kidney ratio: T/K. V: volume.

Supplementary Material

Supplementary figures and tables.

<http://www.thno.org/v08p5106s1.pdf>

Competing Interests

N.K. Cheung reports receiving commercial research grants from Y-mabs Therapeutics and Abpro-Labs Inc.; holding ownership interest/equity in Y-Mabs Therapeutics Inc., holding ownership interest/equity in Abpro-Labs, and owning stock options in Eureka Therapeutics. NKC is the inventor and owner of issued patents both currently unlicensed and licensed by MSK to Ymabs

Therapeutics, Biotec Pharmacon, and Abpro-labs. NKC is an advisory board member for Abpro-Labs and Eureka Therapeutics. SM Larson reports receiving commercial research grants from Genentech, Willex, Telix and Regeneron; holding ownership interest/equity in Voreyda Theranostics Inc. and Elucida Oncology Inc, and holding stock in ImaginAb. SML is the inventor and owner of issued patents both currently unlicensed and licensed by MSK to Samus Therapeutics and Elucida Oncology Inc. SML is or has been consultant to Cynvec, Eli Lilly, Prescient, Advanced Innovative Partners, Gerson Lehrman, Progenics and Janssen Pharmaceuticals. All other authors have no competing interests.

References

- Larson SM, Carrasquillo JA, Cheung NK, Press OW. Radioimmunotherapy of human tumours. *Nat Rev Cancer* 2015; 15: 347-60.
- Kraeber-Bodere F, Rousseau C, Bodet-Milin C, Frampas E, Faivre-Chauvet A, Rauscher A, et al. A pretargeting system for tumor PET imaging and radioimmunotherapy. *Front Pharmacol* 2015; 6: 54.
- Altai M, Membreno R, Cook B, Tolmachev V, Zeglis BM. Pretargeted imaging and therapy. *J Nucl Med* 2017; 58: 1553-9.
- Frampas E, Rousseau C, Bodet-Milin C, Barbet J, Chatal JF, Kraeber-Bodere F. Improvement of radioimmunotherapy using pretargeting. *Front Oncol* 2013; 3: 159.
- Goldenberg DM, Chang CH, Rossi EA, J W, McBride, Sharkey RM. Pretargeted molecular imaging and radioimmunotherapy. *Theranostics* 2012; 2: 523-40.
- Patra M, Zarschler K, Pietzsch HJ, Stephan H, Gasser G. New insights into the pretargeting approach to image and treat tumours. *Chem Soc Rev* 2016; 45: 6415-31.
- Cheal SM, Xu H, Guo HF, Zanzonico PB, Larson SM, Cheung NK. Preclinical evaluation of multistep targeting of disialoganglioside GD2 using an IgG-scFv bispecific antibody with high affinity for GD2 and DOTA metal complex. *Mol Cancer Ther* 2014; 13: 1803-12.
- Cheal SM, Xu H, Guo HF, Lee SG, Punzalan B, Chalasani S, et al. Theranostic pretargeted radioimmunotherapy of colorectal cancer xenografts in mice using picomolar affinity Y-86- or Lu-177-DOTA-Bn binding scFv C825/GPA33 IgG bispecific immunoconjugates. *Eur J Nucl Med Mol Imaging* 2016; 43: 925-37.
- Green DJ, Frayo SL, Lin Y, Hamlin DK, Fisher DR, Frost SH, et al. Comparative analysis of bispecific antibody and streptavidin-targeted radioimmunotherapy for B-cell cancers. *Cancer Res* 2016; 76: 6669-6679.
- Green DJ, O'Steen S, Lin Y, Comstock ML, Kenoyer AL, Hamlin DK, et al. CD38 bispecific antibody pretargeted radioimmunotherapy for multiple myeloma and other B cell malignancies. *Blood*. 2017; 131: 611-620.
- Orcutt KD, Slusarczyk AL, Cieslewicz M, Ruiz-Yi B, Bhushan KR, Frangioni JV, et al. Engineering an antibody with picomolar affinity to DOTA chelates of multiple radionuclides for pretargeted radioimmunotherapy and imaging. *Nucl Med Biol* 2011; 38: 223-33.
- Orcutt KD, Ackerman ME, Cieslewicz M, Quiroz E, Slusarczyk AL, Frangioni JV, et al. A modular IgG-scFv bispecific antibody topology. *Protein Eng Des Sel* 2010; 23: 221-8.
- Orcutt KD, Nasr KA, Whitehead DG, Frangioni JV, Wittrup KD. Biodistribution and clearance of small molecule hapten chelates for pretargeted radioimmunotherapy. *Mol Imaging Biol* 2011; 13: 215-21.
- Orcutt KD, Rhoden JJ, Ruiz-Yi B, Frangioni JV, Wittrup KD. Effect of small-molecule-binding affinity on tumor uptake in vivo: a systematic study using a pretargeted bispecific antibody. *Mol Cancer Ther*. 2012; 11: 1365-72.
- Austin CD, De Maziere AM, Pisacane PI, van Dijk SM, Eigenbrot C, Sliwkowski MX, et al. Endocytosis and sorting of ErbB2 and the site of action of cancer therapeutics trastuzumab and geldanamycin. *Mol Biol Cell* 2004; 15: 5268-82.
- Rudnick SI, Lou J, Shaller CC, Tang Y, Klein-Szanto AJ, Weiner LM, et al. Influence of affinity and antigen internalization on the uptake and penetration of Anti-HER2 antibodies in solid tumors. *Cancer Res* 2011; 71: 2250-9.
- Marks LB, Yorke ED, Jackson A, Ten Haken RK, Constine LS, Eisbruch A, et al. Use of normal tissue complication probability models in the clinic. *Int J Radiat Oncol Biol Phys* 2010; 76: S10-9.
- Pearse G, Frith J, Randall KJ, Klinowska T. Urinary retention and cystitis associated with subcutaneous estradiol pellets in female nude mice. *Toxicol Pathol* 2009; 37: 227-34.
- Yang CH, Almomen A, Wee YS, Jarboe EA, Peterson CM, Janat-Amsbury MM. An estrogen-induced endometrial hyperplasia mouse model recapitulating human disease progression and genetic aberrations. *Cancer Med* 2015; 4: 1039-50.
- Sahota PS (Ed.), Popp JA (Ed.), Hardisty JF (Ed.), Gopinath C (Ed). *Toxicologic pathology: nonclinical safety assessment*. Boca Raton: CRC Press; 2013: 155.
- Menard S, Fortis S, Castiglioni F, Agresti R, Balsari A. HER2 as a prognostic factor in breast cancer. *Oncology*. 2001; 61 Suppl 2: 67-72.
- Jorgensen JT, Hersom M. HER2 as a prognostic marker in gastric cancer - a systematic analysis of data from the literature. *J Cancer* 2012; 3: 137-44.
- English DP, Roque DM, Santin AD. HER2 expression beyond breast cancer: therapeutic implications for gynecologic malignancies. *Mol Diagn Ther* 2013; 17: 85-99.
- Hudis CA. Trastuzumab--mechanism of action and use in clinical practice. *N Engl J Med* 2007; 357: 39-51.
- Bookman MA, Darcy KM, Clarke-Pearson D, Boothby RA, Horowitz IR. Evaluation of monoclonal humanized anti-HER2 antibody, trastuzumab, in patients with recurrent or refractory ovarian or primary peritoneal carcinoma with overexpression of HER2: a phase II trial of the Gynecologic Oncology Group. *J Clin Oncol* 2003; 21: 283-90.
- Vogel CL, Cobleigh MA, Tripathy D, Gutheil JC, Harris LN, Fehrenbacher L, et al. Efficacy and safety of trastuzumab as a single agent in first-line treatment of HER2-overexpressing metastatic breast cancer. *J Clin Oncol* 2002; 20: 719-26.
- Verma S, Miles D, Gianni L, Krop IE, Welslau M, Baselga J, et al. Trastuzumab emtansine for HER2-positive advanced breast cancer. *N Engl J Med* 2012; 367: 1783-91.
- Brechbiel MW, Waldmann TA. Anti-HER2 radioimmunotherapy. *Breast Dis*. 2000; 11: 125-32.
- Rasaneh S, Rajabi H, Akhlaghpour S, Sheybani S. Radioimmunotherapy of mice bearing breast tumors with Lu-177-labeled trastuzumab. *Turk J Med Sci* 2012; 42: 1292-8.
- Abbas N, Bruland OS, Brevik EM, Dahle J. Preclinical evaluation of 227Th-labeled and 177Lu-labeled trastuzumab in mice with HER-2-positive ovarian cancer xenografts. *Nucl Med Commun* 2012; 33: 838-47.
- Ray GL, Baidoo KE, Keller LM, Albert PS, Brechbiel MW, Milenic DE. Pre-clinical assessment of Lu-labeled trastuzumab targeting HER2 for treatment and management of cancer patients with disseminated intraperitoneal disease. *Pharmaceuticals (Basel)* 2011; 5: 1-15.
- D'Huyvetter M, Vincke C, Xavier C, Aerts A, Impens N, Baatout S, et al. Targeted radionuclide therapy with a 177Lu-labeled anti-HER2 nanobody. *Theranostics*. 2014; 4: 708-20.
- Cheal SM, Fung EK, Patel M, Xu H, Guo HF, Zanzonico PB, et al. Curative Multicyclic Radioimmunotherapy Monitored by Quantitative SPECT/CT-Based Theranostics, Using Bispecific Antibody Pretargeting Strategy in Colorectal Cancer. *J Nucl Med* 2017; 58: 1735-42.
- Ram S, Kim D, Ober RJ, Ward ES. The level of HER2 expression is a predictor of antibody-HER2 trafficking behavior in cancer cells. *MABs* 2014; 6: 1211-9.
- Hapuarachchige S, Kato Y, Artemov D. Bioorthogonal two-component drug delivery in HER2(+) breast cancer mouse models. *Sci Rep* 2016; 6: 24298.
- Hapuarachchige S, Zhu W, Kato Y, Artemov D. Bioorthogonal, two-component delivery systems based on antibody and drug-loaded nanocarriers for enhanced internalization of nanotherapeutics. *Biomaterials* 2014; 35: 2346-54.
- Khaw BA, Gada KS, Patil V, Panwar R, Mandapati S, Hatefi A, et al. Bispecific antibody complex pre-targeting and targeted delivery of polymer drug conjugates for imaging and therapy in dual human mammary cancer xenografts: targeted polymer drug conjugates for cancer diagnosis and therapy. *Eur J Nucl Med Mol Imaging* 2014; 41: 1603-16.
- O'Donoghue JA, Bardies M, Wheldon TE. Relationships between tumor size and curability for uniformly targeted therapy with beta-emitting radionuclides. *J Nucl Med* 1995; 36: 1902-9.
- Ljungberg M, Celler A, Konijnenberg MW, Eckerman KF, Dewaraja YK, Sjogreen-Gleisner K, et al. MIRD pamphlet no. 26: joint EANM/MIRD guidelines for quantitative 177Lu SPECT applied for dosimetry of radiopharmaceutical therapy. *J Nucl Med* 2016; 57: 151-62.
- Delker A, Fendler WP, Kratochwil C, Brunegrab A, Gosewisch A, Gildehaus FJ, et al. Dosimetry for (177)Lu-DKFZ-PSMA-617: a new radiopharmaceutical for the treatment of metastatic prostate cancer. *Eur J Nucl Med Mol Imaging* 2016; 43: 42-51.
- Sharkey RM, van Rij CM, Karacay H, Rossi EA, Frielink C, Regino C, et al. A new Tri-Fab bispecific antibody for pretargeting Trop-2-expressing epithelial cancers. *J Nucl Med* 2012; 53: 1625-32.
- van Rij CM, Lutje S, Frielink C, Sharkey RM, Goldenberg DM, Franssen GM, et al. Pretargeted immuno-PET and radioimmunotherapy of prostate cancer with an anti-TROP-2 x anti-HSG bispecific antibody. *Eur J Nucl Med Mol Imaging* 2013; 40: 1377-83.
- Houghton JL, Membreno R, Abdel-Atti D, Cunanan KM, Carlin S, Scholz WW, et al. Establishment of the In Vivo Efficacy of Pretargeted Radioimmunotherapy Utilizing Inverse Electron Demand Diels-Alder Click Chemistry. *Mol Cancer Ther* 2017; 16: 124-33.
- Bodet-Milin C, Ferrer L, Rauscher A, Masson D, Rbahr-Vidal L, Faivre-Chauvet A, et al. Pharmacokinetics and dosimetry studies for optimization of pretargeted radioimmunotherapy in CEA-expressing advanced lung cancer patients. *Front Med (Lausanne)* 2015; 2: 84.
- Schoffelen R, Woliner-van der Weg W, Visser EP, Goldenberg DM, Sharkey RM, McBride WJ, et al. Predictive patient-specific dosimetry and

- individualized dosing of pretargeted radioimmunotherapy in patients with advanced colorectal cancer. *Eur J Nucl Med Mol Imaging* 2014; 41: 1593-602.
46. Weiden PL, Breitz HB, Press O, Appelbaum JW, Bryan JK, Gaffigan S, et al. Pretargeted radioimmunotherapy (PRIT) for treatment of non-Hodgkin's lymphoma (NHL): initial phase I/II study results. *Cancer Biother Radiopharm* 2000; 15: 15-29.
47. Knox SJ, Goris ML, Tempero M, Weiden PL, Gentner L, Breitz H, et al. Phase II trial of yttrium-90-DOTA-biotin pretargeted by NR-LU-10 antibody/streptavidin in patients with metastatic colon cancer. *Clin Cancer Res* 2000; 6: 406-14.
48. Wild D, Fani M, Fischer R, Del Pozzo L, Kaul F, Krebs S, et al. Comparison of somatostatin receptor agonist and antagonist for peptide receptor radionuclide therapy: a pilot study. *J Nucl Med* 2014; 55: 1248-52.
49. Yoon S, Kim YH, Kang SH, Kim SK, Lee HK, Kim H, et al. Bispecific Her2 x cotinine antibody in combination with cotinine-(histidine)₂-iodine for the pre-targeting of Her2-positive breast cancer xenografts. *J Cancer Res Clin Oncol* 2014; 140: 227-33.
50. Carter P, Presta L, Gorman CM, Ridgway JB, Henner D, Wong WL, et al. Humanization of an anti-p185HER2 antibody for human cancer therapy. *Proc Natl Acad Sci USA* 1992; 89: 4285-9.
51. Breitz HB, Durham JS, Fisher DR, Weiden PL, DeNardo GL, Goodgold HM, et al. Pharmacokinetics and normal organ dosimetry following intraperitoneal rhenium-186-labeled monoclonal antibody. *J Nucl Med* 1995; 36: 754-61.
52. Doha FJ, Rahmani S, Rikhtechi P, Rasaneh S, Sheikholislam Z, Shakhosseini S. Development of DOTA-Rituximab to be Labeled with Y-90 for Radioimmunotherapy of B-cell Non-Hodgkin Lymphoma. *Iran J Pharm Res* 2017; 16: 619-29.
53. Salacinski PR, McLean C, Sykes JE, Clement-Jones VV, Lowry PJ. Iodination of proteins, glycoproteins, and peptides using a solid-phase oxidizing agent, 1,3,4,6-tetrachloro-3- α ,6- α -diphenyl glycoluril (Iodogen). *Anal Biochem* 1981; 117: 136-46.